

AFML-TR-76-179

20 J

ADA038071

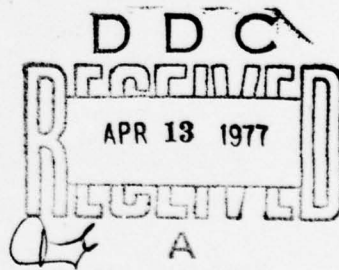
BASIC RESEARCH ON TECHNOLOGY DEVELOPMENT FOR SINTERED CERAMICS

**GENERAL ELECTRIC COMPANY
CORPORATE RESEARCH AND DEVELOPMENT
SCHENECTADY, NEW YORK 12301**

NOVEMBER 1976

**TECHNICAL REPORT AFML-TR-76-179
FINAL REPORT FOR PERIOD 1 AUGUST 1975 - 31 JULY 1976**

Approved for public release; distribution unlimited



NU NU
DDC FILE COPY

AIR FORCE MATERIALS LABORATORY
AIR FORCE WRIGHT AERONAUTICAL LABORATORIES
AIR FORCE SYSTEMS COMMAND
WRIGHT-PATTERSON AIR FORCE BASE, OHIO 45433

NOTICE

When Government drawings, specifications, or other data are used for any purpose other than in connection with a definitely related Government procurement operation, the United States Government thereby incurs no responsibility nor any obligation whatsoever; and the fact that the government may have formulated, furnished, or in any way supplied the said drawings, specifications, or other data, is not to be regarded by implication or otherwise as in any manner licensing the holder or any other person or corporation, or conveying any rights or permission to manufacture, use, or sell any patented invention that may in any way be related thereto.

This report has been reviewed by the Information Office (OI) and is releasable to the National Technical Information Service (NTIS). At NTIS, it will be available to the general public, including foreign nations.

This technical report has been reviewed and is approved for publication.

Norman M Tallan

NORMAN M. TALLAN
Chief, Processing and High
Temperature Materials Branch
Metals and Ceramics Division

FOR THE COMMANDER

Harris M. Burke
HARRIS M. BURKE
Chief, Metals and Ceramics Division
Air Force Materials Laboratory

ACCESSION	FILE
NTIS	
000	
SEARCHED	
INDEXED	
SERIALIZED	
FILED	

A

Copies of this report should not be returned unless return is required by security considerations, contractual obligations, or notice on a specific document.

~~UNCLASSIFIED~~
SECURITY CLASSIFICATION OF THIS PAGE (When Data Entered)

REPORT DOCUMENTATION PAGE		READ INSTRUCTIONS BEFORE COMPLETING FORM
1. REPORT NUMBER AFML-TR-76-179	2. GOVT ACCESSION NO.	3. RECIPIENT'S CATALOG NUMBER
4. TITLE (and Subtitle) BASIC RESEARCH ON TECHNOLOGY DEVELOPMENT FOR SINTERED CERAMICS		5. TYPE OF REPORT & PERIOD COVERED Final Technical Report 1 Aug 1975 - 31 Jul 1976
6. AUTHOR(s) Charles D. Greskovich Svante Prochazka Joseph H. Rosolowski		7. PERFORMING ORG. REPORT NUMBER SRD-76-151
8. CONTRACT OR GRANT NUMBER(S) F33615-76-C-5033 ARPA Order No. 3059 16Y10		9. PERFORMING ORGANIZATION NAME AND ADDRESS General Electric Company Corporate Research and Development Center Schenectady, New York 12301
10. PROGRAM ELEMENT, PROJECT, TASK AREA & WORK UNIT NUMBERS 62712E 30590001		11. CONTROLLING OFFICE NAME AND ADDRESS Air Force Materials Laboratory (LLM) Wright-Patterson Air Force Base, Ohio 45433
12. REPORT DATE November 1976		13. NUMBER OF PAGES 84
14. MONITORING AGENCY NAME & ADDRESS (if different from Controlling Office)		15. SECURITY CLASS. (of this report) Unclassified
16. DISTRIBUTION STATEMENT (of this Report) Approved for public release; distribution unlimited		17. DISTRIBUTION STATEMENT (of the abstract entered in Block 20, if different from Report) 406 (d) 7
18. SUPPLEMENTARY NOTES		
19. KEY WORDS (Continue on reverse side if necessary and identify by block number) Ceramic materials Silicon nitride Sinterable nitrogen ceramics Fugitive sintering aids		
20. ABSTRACT (Continue on reverse side if necessary and identify by block number) Pure silicon nitride powder is prepared by calcination of the reaction product obtained from SiH ₄ and anhydrous NH ₃ at 600°C and above. It is amorphous up to 1480°C and converts to α -Si ₃ N ₄ above this temperature. Hot-pressing at 5 GPa at 1500°C and above yields dense specimens of near theoretical density and up to 3000 kg/m ³ Knoop microhardness (200 g load). Annealing at 1750°C does not induce grain growth. Hot-pressing under nominal conditions up to 1800°C does not bring about appreciable densification.		

DD FORM 1 JAN 73 1473 EDITION OF 1 NOV 65 IS OBSOLETE

UNCLASSIFIED

SECURITY CLASSIFICATION OF THIS PAGE (When Data Entered)

28 degrees

bog

UNCLASSIFIED

SECURITY CLASSIFICATION OF THIS PAGE(When Data Entered)

Exposure of compacts to various atmospheres at 1400-1800°C causes specific surface area reduction and weight loss but no densification. The weight loss is related to specific surface area. Both weight loss and coarsening is related to thermal decomposition of Si_3N_4 . Selected non-oxide additions, on the 1-2% level, permit the attainment of nearly theoretical density in Si_3N_4 by hot-pressing at 1750°-1800°C and sintering at 1800-2000°C. Sintering was done under 8 MPa nitrogen pressure. The dense specimens are composed of $\beta\text{-Si}_3\text{N}_4$ grains having a larger aspect ratio as the sintering temperature is increased. *beta*

UNCLASSIFIED

SECURITY CLASSIFICATION OF THIS PAGE(When Data Entered)

FOREWORD

This research was sponsored by the Advanced Research Projects Agency and carried out in the Physical Chemistry Laboratory of the General Electric Corporate Research and Development Center, Schenectady, New York 12301, under USAF Contract No. F33615-76-C-5033 entitled "Basic Research on Technology Development for Sintered Ceramics," ARPA Order No. 3059, and administered by the Metals and Ceramics Division, Air Force Materials Laboratory, Air Force Wright Aeronaautical Laboratories, Wright-Patterson Air Force Base, Ohio under the direction of Dr. Norman M. Tallan, AFML/LLM.

The work was performed during the period 1 August 1975 to 31 July 1976. It was submitted by the authors on 7 September 1976.

The authors gratefully acknowledge the contribution of W.A. Rocco for high pressure, hot-pressing work, C.O'Clair and C.F. Bobik for their ceramic processing skill, C.W. Krystyniak for the hot-pressing work, M.E. Gill for the SEM work, and D.W. Marsh for X-ray work.

SUMMARY OF IMPORTANT RESULTS

1. Substantial amounts of oxygen contained in submicron particle size silicon nitride cannot be removed by thermal treatment without considerable material loss by evaporation and coarsening due to crystallite growth.
2. Pure ultrafine silicon nitride may be prepared by calcination of the condensation product obtained by heating SiH₄ and anhydrous NH₃ above 500°C. Such Si₃N₄ is amorphous up to 1480°C and converts to the alpha form at this temperature.
3. Si₃N₄ may be densified to near theoretical densities at 5 GPa (800 Kpsi) at 1500°C or above. At lower temperatures limited bonding occurs, as determined by microhardness measurements.
4. Grain growth does not occur on annealing at 1750°C of Si₃N₄ compacts obtained by high-pressure hot-pressing.
5. Relatively pure, submicron Si₃N₄ compacts when heated above 1400°C undergo weight loss and coarsening manifested by surface area reduction. The weight loss is related to the specific surface area and caused, predominantly, by thermal decomposition. Coarsening is brought about by vapor transport due to thermal decomposition and recombination.
6. No shrinkage was observed on Si₃N₄ compacts heated under normal N₂ pressure up to 1800°C. Under 8 MPa of nitrogen (1200 psi) at 2000°C and 2100°C shrinkage does occur but densification is limited.
7. The lack of bonding typical for Si₃N₄ compacts heated at normal nitrogen pressure above 1600°C results from thermal decomposition.
8. Amorphous Si₃N₄ may be hot-pressed under nominal conditions close to theoretical density when sintering promoting additives are used. The most effective additives evaluated in this study were Mg₃N₂, Be₃N₂ and Mg₂Si.
9. On hot-pressing Be₃N₂ addition permits a density maximum at 1-2% and a drop off at higher levels. About 2% of either Mg₃N₂ or Mg₂Si addition yields full density. Higher additions do not have a more pronounced effect on densification but bring about appearance of binary nitride in the X-ray patterns.
10. Sintering with the same additions at normal nitrogen pressure on heating up to 1800°C does bring about some shrinkage, about 5%, however, no densification takes place because of the simultaneous weight loss.

11. Low-green densities obtained with the amorphous powders, thermal decomposition of Si_3N_4 and the limitation of temperature applicable at normal nitrogen pressure are the factors which hinder conventional sintering.
12. At hyperbaric nitrogen pressure sintering of Si_3N_4 to high densities could be achieved with 1% Be_3N_2 and 2% Mg_3N_2 . Ninety-eight percent of theoretical density was obtained at $1880^{\circ}C$ and $2000^{\circ}C$ for amorphous and crystalline Si_3N_4 , respectively.
13. Increased nitrogen pressure decreases the equilibrium pressure of silicon over Si_3N_4 and thus suppresses both thermal decomposition and coarsening due to vapor transport.
14. Si_3N_4 sintered below $1900^{\circ}C$ is composed of β - Si_3N_4 grains 1-2 μ in size both equiaxed and elongated. The microstructure of Si_3N_4 sintered at $2000^{\circ}C$ consists of highly anisotropic β grains 1-3 microns thick and 3-10 μ long.

TABLE OF CONTENTS

Section	Page
I. RESEARCH OBJECTIVES	1
II. GENERAL BACKGROUND	1
III. APPROACH	4
IV. Si_3N_4 POWDER CHARACTERIZATION AND SYNTHESIS	6
A. General	6
B. Characterization of Procured Si_3N_4 Powders	6
1. Physical Data	6
2. Thermal Treatments	8
3. Leaching Treatment	13
4. Summary	15
C. Silicon Nitride Powder Synthesis	15
1. Selection of the Process	15
2. Experimental	16
3. Results	17
4. Discussion	26
5. Summary	29
V. HIGH PRESSURE, HOT PRESSING OF PURE Si_3N_4 POWDERS	30
A. Objective	30
B. Experimental	31
C. Results	35
D. Summary	42
VI. SINTERING BEHAVIOR OF PURE Si_3N_4	43
A. Introduction	43
B. Normal Nitrogen Pressure	43
1. Powder Forming and Firing Conditions	43
2. Characterization of Fired Si_3N_4 Compacts	45
3. Results	45
4. Discussion	48
C. Effect of High Nitrogen Pressures	51
D. Summary	55
VII. HOT-PRESSING OF Si_3N_4 WITH ADDITIVES	57
A. Introduction	57
B. Experimental	57
C. Results and Discussion	58
D. Summary	64

TABLE OF CONTENTS (Cont'd)

Section	Page
VIII. SINTERING OF Si ₃ N ₄ WITH NON-OXIDE ADDITIONS	66
A. General	66
B. Experimental	67
C. Normal Nitrogen Pressure (0.1 MPa) -	
Results	67
D. Sintering of Hyperbasic Nitrogen Pressure	68
1. Results	71
2. Microstructures	74
E. Discussion	79
REFERENCES	82

LIST OF ILLUSTRATIONS

<u>Figure No.</u>		<u>Page No.</u>
1.	Scanning Electron Micrograph of Particles of the SN-402 Si ₃ N ₄ Powder	7
2.	Weight Loss and Specific Surface Area as Function of Temp. for Loose Powder of SN-402 Si ₃ N ₄ Fired in Vacuum for 1 Hr	11
3.	Weight Loss & Specific Surface Area of Loose Powder of SN-402 Si ₃ N ₄ Fired in Dry Hydrogen for 1 Hr	12
4.	Infrared Spectrum for (A) the "As-Received" SN-402 Si ₃ N ₄ Powder, (B) the "As-Received" Si ₃ N ₄ Powder Vacuum-Fired at 1400°C for 1 Hr, (C) the "As-Received" Si ₃ N ₄ Powder Hydrogen-Fired at 1400°C for 1 Hr, (D) the "As-Received" Si ₃ N ₄ Powder Hydrogen-Fired at 1400°C for 1 Hr; then Removed From Furnace, Cooled in Air, and (E) (Cabosil) SiO ₂	14
5.	Surface Area and Density as a Function of Temperature for a Reaction Product SiH ₄ +NH ₃	20
6.	I.R. Absorption Spectra of Reaction Products of SiH ₄ +NH ₃ (A) Synthesized at 600°C, (B) Synthesized at 850°C, (C) Calcined at 1150°C, (D) Calcined at 1480°C, (E) Silicon Rich Product Calcined at 1350°C .	22
7.	Particle Morphology of Amorphous Si ₃ N ₄ Synthesized at 850°C 30,000 X, TEM	24
8.	Electron Diffraction Pattern of Amorphous Si ₃ N ₄	25
9.	Elemental Silicon Inclusion in a Particle of Amorphous Si ₃ N ₄ 300,000 X, TEM	27
10.	Section of a Typical Si ₃ N ₄ Specimen Compacted at 5 GPa and 1550°C	34
11.	TEM of Replica of Fracture Surface of Si ₃ N ₄ Compacted at 5 GPa at 1500°C Specimen No. 2 in Table 4 30,000 X	36

<u>Figure No.</u>	<u>Page No.</u>
12. TEM of Replica of Polished and Etched Surface of Specimen No. 2 White Spots Correspond to Leached Out Silicon Grains 30,000 X	37
13. Hot-Pressed Si_3N_4 (A) As Polished, (B) Same Specimen After Annealing at 1760°C Hr 40 Min Phase Contrast Micrographs, 2000 X	38
14. Microstructure of Poorly Bonded, Hot-Pressed Si_3N_4 (Specimen 5) TEM, Double Stage Replica 30,000 X	39
15. Si_3N_4 (SN-502) Hot-Pressed at 1550°C and 5 GPa SEM of Fracture Surface, (A) 5000 X (B) 10,000 X	40
16. Piece of Specimen 7 (Table 4) Before and After Annealing (Upper Specimen) at 1650°C , 6 X	41
17. Surface of Annealed Specimen 7	42
18. Polished and Etched Surface of Specimen 8 (A) as Prepared at 1500°C (B) Annealed at 1750°C TEM, Double Stage Replica 24,000 X	44
19. Weight Loss and Specific Surface Area as Function of Temp. for (SN-402) Si_3N_4 Compacts Fired for 30 Min in N_2	46
20. Weight Loss and Specific Surface Area as Function of Temp. for (SN-502) Si_3N_4 Compacts Fired for 30 Min in N_2	47
21. Scanning Electron Micrographs of Fractured Surfaces of (SN-402) Compacts Fired 30 Min in N_2 at (A) 1300°C , (B) 1700°C , and (C) 1700°C	49
22. Scanning Electron Micrographs of Fractured Surfaces of (SN-402) Compact Fired at 1850°C for 45 Min in 4.7 MPa (47 atm) of N_2 (A) 2500 X and (B) 10,000 X	54
23. SEM Photomicrograph of Fractured Surface of Si_3N_4 Prepared in Table 1, Exp. No. 3 Mag = 2000 X	56

<u>Figure No.</u>		<u>Page No.</u>
24.	Relative Density of Hot-Pressed Si_3N_4 as Function of Be_3N_2 Content	60
25.	Reflected-Light Photomicrograph of a Polished Section of Hot-Pressed Si_3N_4 Doped with 1 wt% Be_3N_2 Mag = 500 X	61
26.	Relative Density of Hot-Pressed Si_3N_4 as Function of Mg_2Si Content	62
27.	Microstructure of Hot-Pressed Si_3N_4 Doped with 3 wt% Mg_2Si Mag = 500 X	63
28.	Microstructure of Hot-Pressed Si_3N_4 Doped with 2 wt% Mg_3N_2 $T=1750^\circ\text{C}$, $t=20$ min, $p=8000$ psi	64
29.	SEM Photomicrograph of Microstructure of a Compact of SN-402 Si_3N_4 Containing 1 wt% B Fired at 1800°C for 30 min in N_2 (A) 5500 X and (B) 22,000 X	69
30.	SEM Photomicrograph of Microstructure of a Compact of Run (8-10) Si_3N_4 Containing 3 wt% Mg_2Si Fired at 1750°C - 15 Min - N_2 Mag = 5000 X	70
31.	Sintered Si_3N_4 . Disruption of Specimen Due to Amorphous-Crystalline Transition 55 X . .	73
32.	First Si_3N_4 Specimen Sintered to Appreciable Density (Exp. No. 6, Table 8) (A.) Optical Micrograph of Section 580 X . . (B.) SEM of Fracture Surface 10,000 X . .	75
33.	Si_3N_4 Sintered at 1880°C and 8 MPa N_2 to 98% Density 500 X	76
34.	SEM of Polished Section of Specimen No. 13 2200 X	76
35.	Section of Specimen 13 Etched with NaOH Incident Light, 580 X	77
36.	Surface of Overetched Specimen 13 SEM, 2200 X	78
37.	Morphology of Grains in Si_3N_4 Sintered at 2000°C SEM, 10,000 X	78

LIST OF TABLES

<u>TABLE NO.</u>		<u>PAGE NO.</u>
1.	THE EFFECT OF HEAT TREATMENT IN VACUUM AND HYDROGEN ON WEIGHT LOSS, SPECIFIC SURFACE AREA AND OXYGEN CONTENT OF Si_3N_4 POWDER (SN-402)	10
2.	REACTION CONDITIONS AND CHARACTERIZATION OF Si_3N_4 POWDERS SYNTHESIZED FROM SILANE AND AMMONIA	18
3.	I.R. ABSORPTION BANDS IN Si_3N_4 PREPARED AT VARIOUS TEMPERATURES	23
4.	RESULTS OF HOT PRESSING OF Si_3N_4 AT 5 GPa . .	33
5.	RESULTS ON SINTERING Si_3N_4 UNDER HIGH NITROGEN PRESSURE	52
6.	RESULTS FOR HOT PRESSED, DOPED Si_3N_4	59
7.	CHARACTERISTIC TEMPERATURE FOR THE ONSET OF DENSIFICATION DURING HOT PRESSING OF DOPED Si_3N_4	65
8.	RESULTS OF HYPERBARIC SINTERING EXPERIMENTS .	72

SECTION I

RESEARCH OBJECTIVES

The objectives of this research program are to identify the factors which govern the sintering of covalent ceramics, specifically Si_3N_4 , and to apply this knowledge towards developing procedures for sintering dense Si_3N_4 into components suitable for use in high temperature engines. In order to meet these objectives, experiments have been conducted to elucidate which physical and chemical processes prevent or aid the densification of Si_3N_4 and to determine by what means these processes may be appropriately modified, if necessary.

The main thrust of this research is aimed at attempting to densify pure or doped Si_3N_4 by a solid state sintering process. The ability to prepare dense Si_3N_4 with strength levels adequate for turbine parts by sintering would greatly enhance the prospects for fabrication of truly high performance ceramics for high temperature engine applications.

SECTION II

GENERAL BACKGROUND

Silicon nitride is a prime candidate material for high temperature, structural applications. It is, however, a material in which the atomic species exhibit a high degree of covalent bonding, and similar to many other materials (B_4C , AlN , SiC), presents many severe obstacles to its consolidation into useable dense, high strength structures. Hot pressing, chemical vapor deposition (CVD), and recently, sintering processes have been utilized to prepare dense silicon nitride ceramics.

CVD is the only technique found to date to yield fully dense, phase-pure polycrystalline Si_3N_4 in thicknesses up to about 1 mm. Serious problems exist with intergranular cracking, preferred orientation and residual silicon particles. This process is unlikely, however, to be developed in the foreseeable future into a technique for fabrication of components.

The most common fabrication method of producing dense Si_3N_4 is by hot pressing in the presence of a densification aid. Early forms of hot pressed Si_3N_4 contained $\sim 5\text{wt\%}$ MgO and suffered from unacceptably high creep rates and strength degradation at temperatures above 1100°C . The nature of these processes has been

linked to the large addition of the densifying aid, MgO, and to impurity elements (Ca, Fe, Al) in the starting Si_3N_4 powder. It is generally accepted that a thin, amorphous (glassy) intergranular phase controls the high temperature mechanical properties of Si_3N_4 by a grain boundary sliding effect. Calcium magnesium silicate⁽¹⁾ and calcium aluminum silicate⁽²⁾ have been identified in the microstructure by Auger spectroscopy. By reducing the MgO additive to about 2 wt% and the Ca content to about 0.07 wt%, the high temperature potential of this hot pressed form of Si_3N_4 was shifted to about 1200°C.

Further improvements in the high temperature mechanical stability of Si_3N_4 is currently being sought by the replacement of MgO with other oxide additives such as Y_2O_3 ⁽³⁾, CeO_2 ⁽⁴⁾, Ce_2O_3 ⁽⁴⁾ and ZrO_2 ⁽⁵⁾. These additions are believed to result in the formation of more refractory silicate or oxynitride phases which aid densification and are more stable at high temperatures. For example, $\text{Y}_2\text{Si}_3\text{O}_3\text{N}_4$ is a reaction product detected when 5 wt% Y_2O_3 is added to Si_3N_4 , presintered to about 1700°C and then hot pressed at 1750°C at 98 kPa⁽⁶⁾. The high values ($\sim 50 \text{ J/m}^2$) of fracture energy frequently observed in this material are probably related to the polyphase nature of this ceramic⁽⁷⁾. However, one can anticipate some problems in the use of such polyphase Si_3N_4 bodies:

- (1) The polyphase microstructure will have incoherent grain boundaries and exhibit thermal expansion mismatch; consequently, microcracking may result, especially on thermal cycling.
- (2) The relatively large oxide additions necessary to promote densification will result in decreased thermal conductivity offsetting the benefit of the low thermal expansion coefficient ($\sim 3 \times 10^{-6} \text{ }^\circ\text{C}^{-1}$) of relatively pure Si_3N_4 under thermal stress conditions.
- (3) Crystalline silicates MgSiO_3 and $\text{MgO} \cdot \text{CaO} \cdot 2\text{SiO}_2$, form, for example, during oxidation of conventional hot pressed doped Si_3N_4 ⁽⁸⁾. The protective effect of this type of surface oxide films may be strongly affected under thermal cycling conditions. Furthermore, as Lange⁽⁹⁾ has recently shown, subtle compositional changes may result in catastrophic oxidation of bodies in the Si_3N_4 - Y_2O_3 system.

The recent successful consolidation of Si_3N_4 by the sintering process has been a major advance towards the fabrication of complex shapes. Under specific conditions Si_3N_4 with ~ 5 wt% MgO was densified to relative densities greater than 90%^(10,11). The fracture stress versus temperature curves for sintered and hot pressed Si_3N_4 are found to have the same shape, with a marked reduction in strength occurring at about 1000°C⁽¹²⁾. This information suggests that an amorphous, grain boundary silicate phase also exists in this form of sintered Si_3N_4 and controls the

high temperature, mechanical, and oxidation properties. A major problem during sintering is found to be the thermal decomposition of Si_3N_4 which leads to evaporation and lower final densities. Preliminary experiments showed that partial control of thermal decomposition could be accomplished through the use of high nitrogen pressures(11).

Quite recently, sintered densities of 98% and room temperature flexural strength of 100 Kpsi have been obtained by Buljan and Kleiner of GTE Sylvania(13) and Tsao Oda of NGK(14). Both of these latter disclosures refer to proprietary processes and not enough information is available to assess their potential. As long as oxide sintering additions are used, however, there is no reason to expect better high temperature performance than in the hot pressed forms of silicon nitride.

Reaction sintering is the oldest and best known consolidation technique for Si_3N_4 and is being studied by many groups around the world. The absence of shrinkage and the great versatility in shaping make it particularly attractive for Si_3N_4 component fabrication. The practically achievable density upon nitridation of preshaped silicon powder compacts is, however, limited to between 70 and 80%. Consequently, the strength of typical test bars of about $0.3 \times 0.3 \times 2.5$ cm does not exceed 280 MPa, a value not sufficient for many typical applications. The strength limitation arises from several circumstances:

- (1) Green densities over 65% are required if final densities are to exceed 80% of the theoretical density. Current ceramic processes will not yield this degree of densification with a 5 micron silicon powder.
- (2) Cessation of silicon nitridation is observed when the density reaches about 80%; thus, when nitridation of a silicon compact of $\sim 65\%$ density is attempted (such as obtained by flame spraying), a silicon-silicon nitride body is formed. Cracking may occur due to stresses resulting from the molar volume change (+22%) upon nitridation if the forming Si_3N_4 cannot be accommodated in the available pore space. From available data, the mean strength increases with nitrided density and is controlled by the largest effective pore size and probably, by other yet unidentified parameters(15).

Therefore, a process of consolidation of Si_3N_4 to produce ceramic components for load bearing applications at $\sim 1400^\circ\text{C}$ is not currently available. This report discusses our approach towards achieving this goal.

SECTION III

APPROACH

Two years ago the Ceramics Branch of the General Electric Corporate Research and Development Center initiated a program to (1) investigate some of the intrinsic properties of pure Si_3N_4 by studying the creep and oxidation resistance of high quality CVD foils; the results obtained would tell whether or not Si_3N_4 could meet the high temperature specifications projected for use at 1400°C , and (2) identify the important factors which control the sintering behavior of covalently-bonded solids, especially $\beta\text{-SiC}$ and Si, about which some information was available, so that the theoretical and experimental findings could be applied to the sintering of a very intractable material, Si_3N_4 . The results of this investigation may be summarized as follows⁽¹⁶⁾:

- (1) Creep experiments on CVD foils of Si_3N_4 in three point bending at $\sim 1540^\circ\text{C}$ showed essentially no deflection after 7×10^5 sec at 70 MPa. The material exhibited an upper creep limit of $\sim 10^{-11} \text{ sec}^{-1}$ outer fiber strain or a creep rate at least 5 orders of magnitude less than that expected for commercially hot-pressed Si_3N_4 containing MgO, based on extrapolation from published data.
- (2) Oxidation studies monitored by weight gain measurements showed a rate of $10^{-4} \text{ kg/m}^2\text{s}^{\frac{1}{2}}$ at 1450°C , or about 10 times less than Si_3N_4 hot pressed with 5% MgO and tested at $\sim 1100^\circ\text{C}$.
- (3) Although the specific grain structure found in CVD material makes generalizations of these results to a polycrystalline Si_3N_4 somewhat uncertain, it can be concluded that the intrinsic potential of Si_3N_4 as a high temperature structural material is indeed excellent.
- (4) The mechanism proposed to explain the microstructure that develops in unsinterable covalent solids which does not undergo a phase change is based on the existence of a high ratio of surface and/or vapor-phase matter transport-to-volume and/or grain-boundary transport.
- (5) The addition of a nonoxide sintering aid, boron, to both $\beta\text{-SiC}$ - and Si-containing carbon, retards surface and/or vapor-phase transport and grain growth at lower temperatures, which results in enhanced densification at high temperatures.
- (6) The sintering of pure Si depends sensitively on particle size in the submicron range. Theoretical density is nearly achieved at 1375°C by using 0.06 micron silicon powder.

(7) Finally, the ability to sinter submicron silicon powder compacts to any desired density opened up a new approach to reaction sintering; the nitridation of a sintered pre-form of pure or doped silicon having any desired initial density.

The establishment of the unique high temperature properties of pure Si_3N_4 described above, coupled with the elucidation of the important parameters which must be controlled for the sintering of covalently-bonded solids, led to the present approach of attempting to densify pure and doped- Si_3N_4 under the ARPA/AFML (Contract No. F33615-76-C-5033) program initiated in 1975.

Experience indicates that there exist four main obstacles which hinder the application of solid state sintering principles to the densification of Si_3N_4 without property degrading phases and additives. First, the decomposition temperature of Si_3N_4 is only around 1900°C at 0.1 MPa (1 atm) of nitrogen, and therefore large weight losses by vaporization and thermal decomposition are anticipated and observed. This characteristic suggests that ultrafine particle size Si_3N_4 powders must be prepared and utilized to enhance volume and/or grain boundary diffusion at somewhat lower temperatures. Secondly, this characteristic virtually demands that high nitrogen pressures, perhaps in the kilobar range may be required to suppress decomposition. A third obstacle is the judicious search and use of solute additives to achieve matter transport mobility sufficient to promote grain boundary formation, yet insufficient to significantly degrade high temperature properties. Finally, the $\alpha \rightarrow \beta$ Si_3N_4 transformation, which may lead to elongated grain morphologies and bridging particle structures before densification is complete, is considered to be undesirable, and means should be sought for its inhibition or control.

With the background developed during the first year and with experience acquired in prior sintering work, the following objectives were sought in order to elucidate the possibility of fabricating dense Si_3N_4 with potentially improved properties:

- (1) Provide and characterize a source of silicon nitride powder with highest possible purity, especially with respect to oxygen, free silicon and other metals. The ultimate particle size should be in the 0.1 micron range, and have a low degree of crystallinity.
- (2) Obtain information, by some indirect means, on the atomic mobility in pure Si_3N_4 to assess the temperature range at which densification could be observed, in principle.
- (3) Study the behavior of pure Si_3N_4 powders and its particle morphology under various heat treatment conditions to determine whether bonding and neck formation occurs, and which of the above listed obstacles might interfere with densification.

- (4) Study the effect of small additions of selected non-oxide substances on the bonding and densification of Si_3N_4 and identify those with promoting effects. Emphasize those substances, which are unlikely to bring about melt formation.
- (5) Optimize the sintering process to obtain high density ceramics and fine-grained microstructures.

The following chapters describe and discuss work done along these lines. The approach was successful and conditions for sintering Si_3N_4 to high densities have been identified. However, continuing effort is necessary to further investigate and optimize the process, and evaluate the resulting Si_3N_4 bodies.

SECTION IV

Si_3N_4 POWDER CHARACTERIZATION AND SYNTHESIS

A. General

It has been shown in previous work that the ultimate particle size of covalent solids, such as SiC and Si , must be extremely small in order to induce sintering. Crystalline sizes well in the submicron range are required. In addition, high chemical purity and a low degree of crystallinity are also believed to be necessary characteristics. The only Si_3N_4 with specifications close to these available at the beginning of this contract, was GTE Sylvania's SN-402 (amorphous) and SN-502 (crystalline) powders. After initial delivery of one pound lots of these materials, however, the supplier withdrew these products from the market. Consequently, further work with Sylvania's silicon nitride powders was terminated and work during the second half of the year was based on Si_3N_4 powder prepared "In-House". The use of other Si_3N_4 powders, such as those marketed by AME*, have not been considered because of the high impurity levels of iron, calcium, aluminum, oxygen and free silicon. The following sections present work done on characterization and attempts at oxygen removal of GTE Sylvania's powders and the synthesis of our own Si_3N_4 powders.

B. Characterization of Procured Si_3N_4 Powders

1. Physical Data

The powder, identified as SN-402, was primarily amorphous and had a purity >99.99% by weight with respect to

*Advanced Materials Engineering, Durham, England

metallic contamination. The major metallic impurity was molybdenum, 0.01 wt%. An oxygen content of 3.14 wt% was measured by neutron activation analysis, and agrees well with the value of ~3 wt% measured by the supplier. X-ray fluorescence revealed the presence of about 1 wt% Cl, a value in agreement with that given by the supplier. The chlorine contamination apparently arises from the synthesis of Si_3N_4 by the reaction between SiCl_4 and NH_3 . X-ray diffraction analysis using a Debye-Scherrer camera and 5×10^4 sec of exposure time showed that the SN-402 powder contained a trace amount of $\alpha\text{-Si}_3\text{N}_4$, a trace of free silicon, and no crystalline or amorphous SiO_2 or ammonium chloride. Also, there were very weak, unidentified diffraction lines at d-spacings of 5.60 Å, 3.29 Å, 2.17 Å and 2.63 Å, which may indicate possible traces of some (Mo,Cr) silicides. The lattice parameters of the $\alpha\text{-Si}_3\text{N}_4$ were $a_0 = 7.752$ Å and $c_0 = 5.614$ Å.

The particle size and shape were determined by specific surface area measurements and observations by scanning electron microscopy (SEM). The SEM photomicrograph presented in Figure 1 shows that the powder particles are uniformly equiaxed, having a size of about 0.2 μ , and appear to be at least partially aggregated.

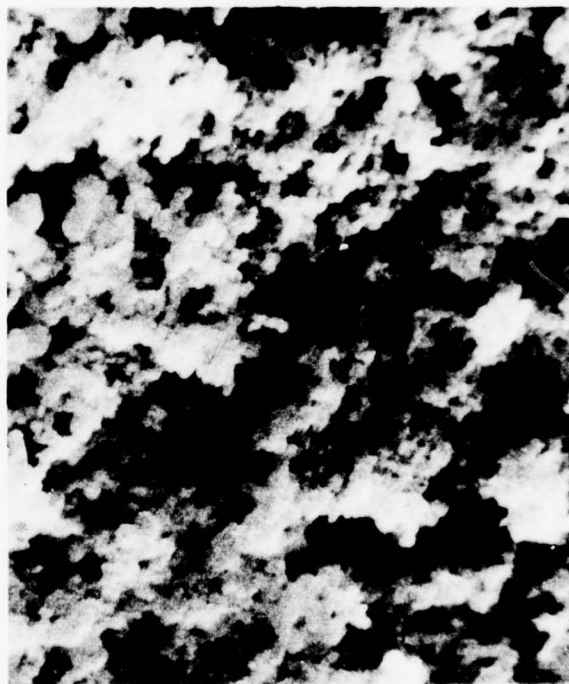


Figure 1. Scanning Electron Micrograph of Particles of the SN-402 Si_3N_4 Powder

The specific surface area, measured by the single point B.E.T. method, was $12.8 \text{ m}^2/\text{g}$ and corresponds to an average ultimate particle size of 0.15μ . The B.E.T. method is, of course, a more reliable method of measuring the average particle size of submicron powders than is SEM.

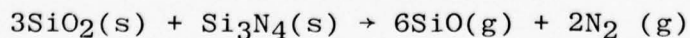
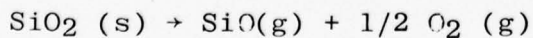
The second Si_3N_4 powder purchased from GTE Sylvania was identified as SN-502. This powder had a purity greater than 99.9% with molybdenum being the major metallic contaminant of about 0.01 wt%. The oxygen and chlorine content of this powder were 1 wt% and <0.04 wt%, respectively. This SN-502 powder was crystalline, as determined by X-ray diffraction analysis, and contained about 94% α - Si_3N_4 and 6% β - Si_3N_4 . Forms of SiO_2 or Si_2ON_2 could not be detected by X-ray analysis. The lattice parameters of the α - Si_3N_4 were nearly the same as that measured for the α - Si_3N_4 phase in the SN-402 powder.

The average particle size, as determined from the specific surface area measurement of $4.5 \text{ m}^2/\text{g}$, was 0.42μ . Particles of α - Si_3N_4 were equiaxed, but some were elongated with aspect ratios as high as 20:1. It is believed that the anisotropic crystallites are β - Si_3N_4 .

2. Thermal Treatments

The high oxygen content of ~ 3 wt% in the starting Si_3N_4 powder is believed to be undesirable since its presence can lead to formation of silicate phases in the fired material which have deleterious effects on high temperature mechanical properties. Wright and Niesz⁽¹⁷⁾ reported that as much as 50% of the oxygen could be removed by thermal treatment at 1600°C under a nitrogen pressure of 4 kPa (30 torr) for several types of starting powder. These powders had initial specific surface areas between 2 and $4 \text{ m}^2/\text{g}$, and particle growth and aggregation occurred during firing which reduced the sinterability of the starting powder. The powder used in this present study, SN-402, has a specific surface area of $12 \text{ m}^2/\text{g}$ and is about 4 times finer than those powders investigated by Wright and Niesz. The application of a preliminary heat treatment schedule was found to cause a 75% reduction in the specific surface area of the powder and significantly reduce the sinterability of the powder. Consequently, other heat treatment schedules were explored.

The removal of oxygen from Si_3N_4 powders at high temperatures probably occurs by one or both of the following possible chemical reactions:



The oxygen is assumed to be present primarily in the form of discrete SiO_2 particles, (SiO_2 particles are observed in polished sections of dense samples prepared from SN-402 and SN-502 Si_3N_4 powders formed under diamond-forming conditions), or in the form of a passivation layer of SiO_2 surrounding the Si_3N_4 particles. In the latter case, reaction can occur at the $\text{Si}_3\text{N}_4/\text{SiO}_2$ interface with the formation of SiO and N_2 gases. This reaction can proceed at a reasonable rate only if the product gases escape.

By using the free energies of formation available in the JANAF tables⁽¹⁸⁾, calculations reveal that for reaction (1) at 1700°K

$$P_{\text{SiO}} \cdot P_{\text{O}_2}^{\frac{1}{2}} = 6.5 \times 10^{-12}$$

and for reaction (2) at 1700°K

$$P_{\text{SiO}}^6 \cdot P_{\text{N}_2}^2 = 8 \times 10^{-18}$$

These calculations show that by firing the starting powder in dry H_2 (dew point = -60°C) the partial pressure of oxygen is 5 fPa (5×10^{-20} atm) at 1700°K. Consequently, there is a strong tendency to form SiO gas, $P_{\text{SiO}} \approx 3\text{kPa}$ (3×10^{-2} atm), by reaction (1). Reaction (2) should also proceed during hydrogen firing or when H_2/N_2 mixtures or vacuum are used. Furthermore, by firing in a vacuum of 1.3 mPa where the P_{O_2} is ~0.3 mPa and the P_{N_2} is ~1 mPa, there will also be a tendency to form SiO gas by reaction (1).

The results of the effect of hydrogen and vacuum firing on weight loss, specific surface area, and residual oxygen content of SN-402 Si_3N_4 powder, are presented in Table 1 and Figures 2 and 3.

In both firing treatments, 5 grams of Si_3N_4 powder was spread out on a tungsten sheet in an identical manner and then fired in a tungsten furnace. Over the temperature range investigated, the weight loss increased and the specific surface area decreased with increasing temperature. The oxygen content was reduced from 3.14 to 0.7 wt% by firing under vacuum (1.3 mPa) for 1 hr at 1400°C, representing a 78% reduction in the oxygen content of the powder. The disadvantages of this heat treatment schedule are that the specific surface area decreases from 13 to 5.8 m^2/g and the weight loss is very high, near 30%. This high weight loss can only be accounted for by the thermal decomposition of Si_3N_4 into Si and N_2 (the equilibrium $P_{\text{N}_2} = 130 \text{ Pa}$ (1.3×10^{-3}

TABLE 1. THE EFFECT OF HEAT TREATMENT IN VACUUM AND
HYDROGEN ON WEIGHT LOSS, SPECIFIC SURFACE AREA AND
OXYGEN CONTENT OF Si_3N_4 POWDER (SN-402)

<u>Heat Treatment</u>	<u>$\Delta W/W_0$ (%)</u>	<u>$S(\text{m}^2/\text{g})$</u>	<u>Oxygen Content* (%)</u>
None	0	13	3.14
1200°C-1 hr-Vac	1.8	12	N.D.
1300°C-1 hr-Vac	10.5	10.7	2.40
1400°C-1 hr-Vac	29	5.8	0.70
1300°C-1 hr- H_2	1.0	12	3.15
1400°C-1 hr- H_2	3.2	10.8	3.05
1500°C-1 hr- H_2	18	8.8	2.48

N.D. = Not Determined

* Neutron Activation Analysis

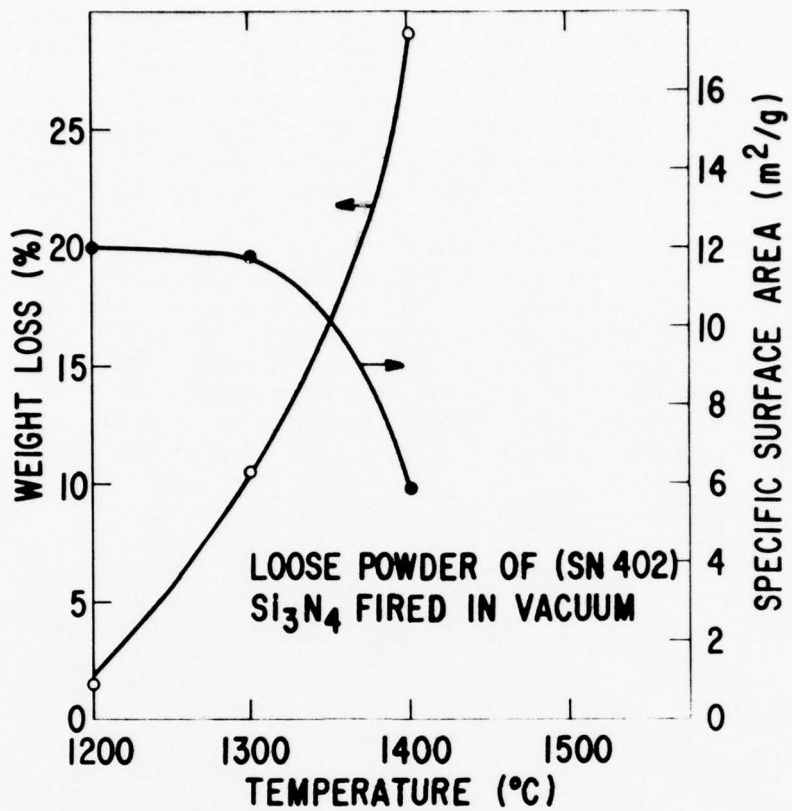


Figure 2. Weight Loss and Specific Surface Area as Function of Temp. for Loose Powder of SN-402 Si_3N_4 Fired in Vacuum for 1 Hr

atm at 1700°K), because the maximum weight loss expected for the SN-402 powder containing ~3 wt% oxygen is about 5.6 wt% according to reaction (1) and 10 wt% according to reaction (2), assuming all the oxygen is removed and no other weight loss mechanisms exist. By firing for 1 hr in dry H_2 at 1500°C, the oxygen content was reduced from 3.14 to 2.48%. A large weight loss of 18% occurred and depended on the thickness of the powder bed used, with smaller weight losses being observed for thicker powder beds. The specific surface area of the Si_3N_4 powder heat treated in hydrogen was always higher than that treated in vacuum at temperatures above 1300°C and attained a value of $8.8 \text{ m}^2/\text{g}$ at 1500°C, corresponding to a 32% reduction in the surface area.

The primarily amorphous Si_3N_4 (SN-402) powder remained white when fired in H_2 at 1300°C and 1400°C, but

turned light grey in color when fired at 1500°C. Under vacuum conditions, the powder was essentially white at 1200°C but turned pale yellow at the higher temperatures. X-ray diffraction analysis showed that powder fired at or above 1400°C consisted primarily of α -Si₃N₄, which was more poorly crystallized when hydrogen-treated rather than vacuum-treated. A small percentage (~5-10%) of poorly crystallized β -Si₃N₄ and a slight trace of free Si were detected in powder vacuum-fired at 1400°C.

It was first thought that changes in oxygen content produced by a given thermal treatment might be detected by infrared spectroscopy. After a specific thermal treatment, the Si₃N₄ powder was placed in a N₂ glove box, weighed in a proportion of 2 mg of Si₃N₄/g KBr, and the mixture pressed into a thin, transparent disc for infrared analysis. Infrared absorption spectra are given in Figures 4(A-E). The spectrum for the "As-

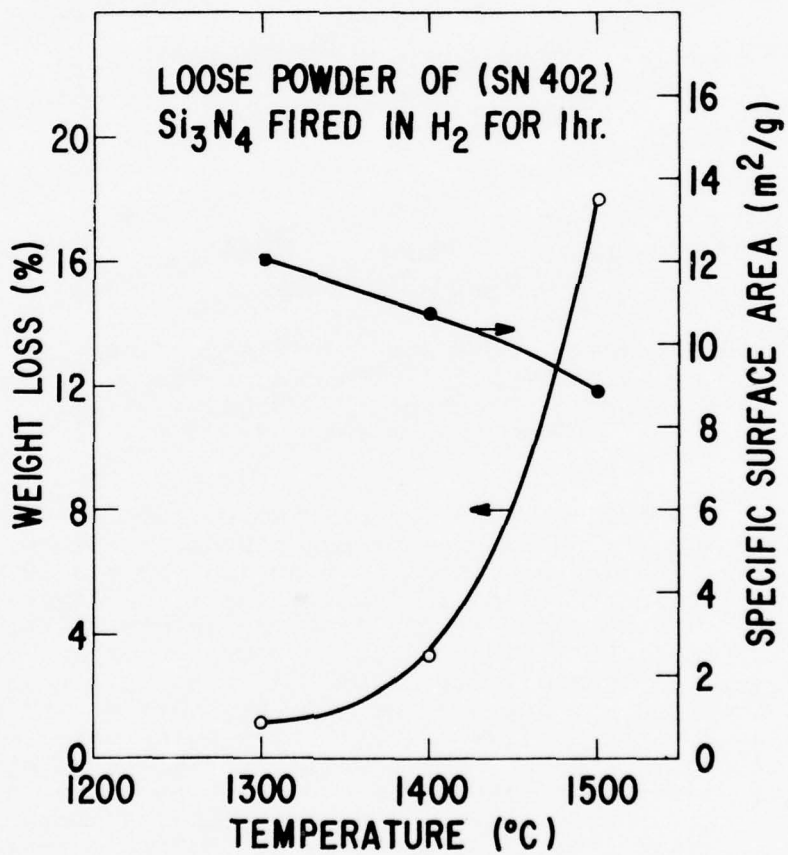


Figure 3. Weight Loss and Specific Surface Area of Loose Powder of SN-402 Si₃N₄ Fired in Dry Hydrogen for 1 Hr

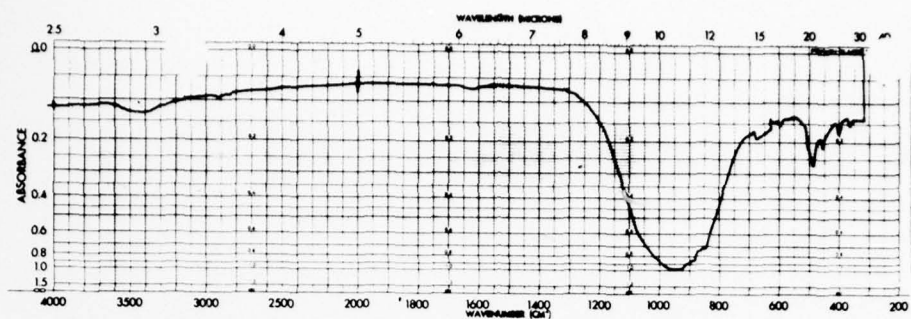
received", primarily amorphous Si_3N_4 (SN-402) powder which contains 3.14 wt% oxygen, is illustrated in Figure 4(A). Small absorption bands located at approximately 2.9 and 6.2 microns are due to vibrations of O-H bonds and arise because of the presence of H_2O in the KBr material. A large broad absorption band due to Si-N vibrations is centered at about 10.5 microns, containing some fine structure between the wavelengths of 11 and 12 microns. Absorption bands also exist at wavelengths beyond approximately 14 microns, but they are less intense and sharp. There is no observable absorption due to Si-O bonds. As illustrated in Figure 4(E) for amorphous SiO_2 , the major Si-O absorption bands occur between about 8 and 10 microns, and if weak, will be masked by the much stronger Si-N absorption band(s) centered at 10.5 microns. The infrared absorption spectrum of powder fired in vacuum at 1400°C and containing only 0.7 wt% oxygen is given in Figure 4(B). All the absorption bands related to the Si_3N_4 structure appear to be sharper and may be attributed to the better crystallinity ($\alpha\text{-Si}_3\text{N}_4$) of the vacuum-fired, Si_3N_4 powder as compared to the amorphous starting powder. The interpretation is further reinforced by comparing this spectrum to that for powder fired at 1400°C in hydrogen (Figure 4(C)). This hydrogen-fired powder, which is composed of poorly crystallized $\alpha\text{-Si}_3\text{N}_4$ and contains nearly 3 wt% oxygen, also shows the same large, broad peak as observed for the "amorphous powder illustrated in Figure 4(A) and no detectable absorption attributable to Si-O bonding. By accident, there was only one case where oxygen was detected in Si_3N_4 powder by infrared spectroscopy. This occurred when Si_3N_4 powder was fired in hydrogen at 1400°C and then removed from the furnace while still hot, and cooled in air. The spectrum of this powder, as seen in Figure 4(D), shows two shoulders on the main absorption band between 8 and 10 microns which agree well with the positions of the Si-O absorption bands for SiO_2 shown in Figure 4(E). The oxygen content of this Si_3N_4 was not determined. The above results demonstrate that infrared spectroscopy cannot be conveniently used to measure small oxygen contents in Si_3N_4 powders, probably less than 5 wt% oxygen.

3. Leaching Treatment

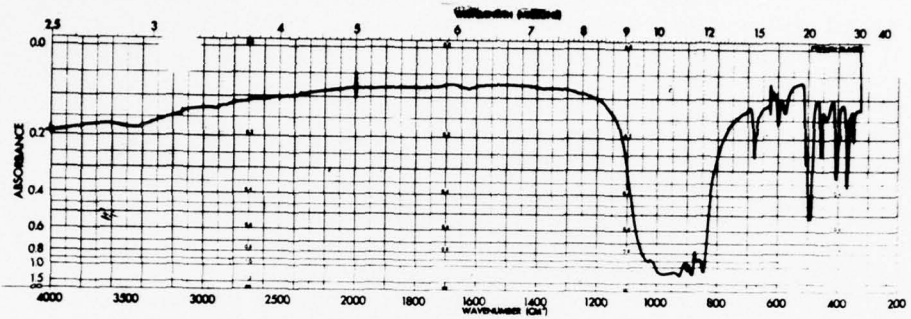
A few experiments were carried out to determine if it was feasible to dissolve the SiO_2 phase from the amorphous (SN-402) Si_3N_4 powder. Sixteen milliliters of concentrated HF was added to a water slurry (1.6 g Si_3N_4 /16 ml) in a teflon beaker, until the onset of gas bubble formation. A strong exothermic reaction occurred. After 3 min the system was heavily diluted with distilled

BEST AVAILABLE COPY

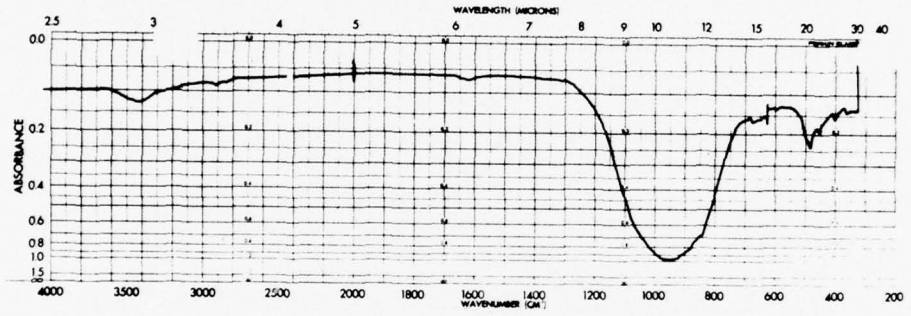
A



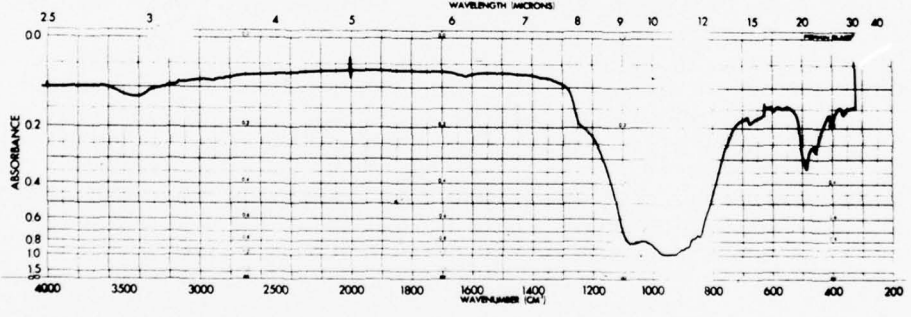
B



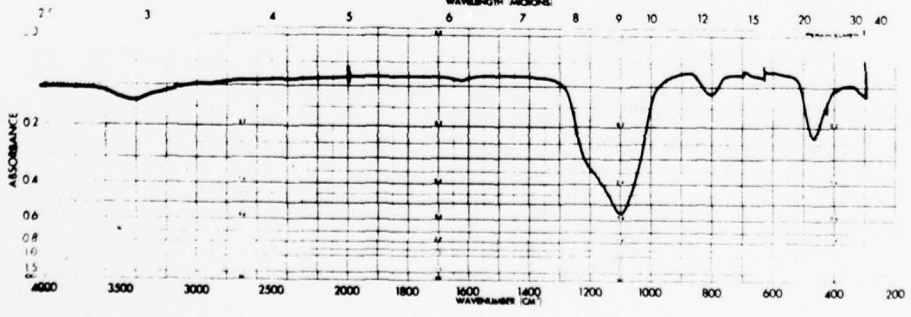
C



D



E



water and filtered and washed. The percent recovery was only 5%, obviously indicating that Si_3N_4 also dissolves in the reagent. In order to suppress the dissolution of Si_3N_4 , the leaching time was decreased by diluting the system at the time when the first gas bubbles were visually observed. The percent of the powder recovered in this case was only 25%. The specific surface area of this leached powder was $10.8 \text{ m}^2/\text{g}$ which is significantly lower than that ($13 \text{ m}^2/\text{g}$) of the starting powder. By considering the reactivity of amorphous Si_3N_4 with HF and the observation that the oxygen content of the leached powder is 2%, as compared to a value of 3.14 wt% for the unleached powder, it appears that leaching with HF acid is not a viable method of significantly reducing the oxygen content, certainly with amorphous Si_3N_4 .

4. Summary

The thermal and leaching experiments conducted on the removal of oxygen from a Si_3N_4 powder of high specific surface area ($13 \text{ m}^2/\text{g}$), strongly indicate that it is extremely difficult to remove a large fraction ($>80\%$) of the oxygen without sacrificing large amounts of material and/or considerable reduction in the specific surface area. Based on the premise that oxygen (SiO_2) in the starting powder is mostly responsible for the formation of undesirable silicate phases which degrade the high temperature, mechanical properties of dense Si_3N_4 , it becomes apparent that the best method of controlling the oxygen content in fine Si_3N_4 powders is by careful powder preparation and processing.

C. Silicon Nitride Powder Synthesis

1. Selection of the Process

Nitridation of crystalline silicon, although it is the most current method of preparing Si_3N_4 , has not been considered, since it does not yield a product with the desired physiochemical characteristics. A number of chemical reactions leading to Si_3N_4 have been described in the literature, such as nitridation of silicon vapor, pyrolysis of silicon diimide(19), synthesis from SiCl_4 ,

Figure 4. Infrared Spectrum for (A) the "As-Received" SN-402 Si_3N_4 Powder, (B) the "As-Received" Si_3N_4 Powder Vacuum-Fired at 1400°C for 1 Hr, (C) the "As-Received" Si_3N_4 Powder Hydrogen-Fired at 1400°C for 1 Hr, (D) the "As-Received" Si_3N_4 Powder Hydrogen-Fired at 1400°C for 1 Hr, Then Removed From Furnace, Cooled in Air, and (E) (Cabosil) SiO_2

N_2 and H_2 ⁽²⁰⁾ or $SiF_4 + NH_3$. Except for the first, which is a demanding high temperature process, these processes start with silicon halides and yield products containing varying amounts of halogens. Morgan⁽²¹⁾ studied one of these processes and found that unless ammonium chloride was completely removed from the intermediates, the resulting Si_3N_4 always contained chlorine. However, the separation of NH_4Cl from $Si(NH_2)_2$ by washing with liquid ammonia, as practiced by Morgan, turned out to be prohibitively slow and expensive. He also observed that residual chlorine in amorphous Si_3N_4 strongly inhibited densification under hot-pressing conditions. Because of this suspected role of halogens in densification of Si_3N_4 , we decided to investigate the synthesis of Si_3N_4 from silane and ammonia. Such a process should circumvent, entirely, the problem of halogen contamination of the resulting Si_3N_4 .

Silane does not react with NH_3 at ambient temperatures, but does react with liquid NH_3 when the reaction is catalyzed by an alkali amide. The product is a condensed substance with a variable composition containing the compounds $Si(NH_2)_2NH$ and $Si(NH_2)_2$. These compounds are very sensitive to moisture, and on contact with ambient air tend to hydrolyze rapidly. Also, the washing of the precipitate with liquid ammonia (to remove the alkali amide) makes this reaction inconvenient as a preparative technique. Therefore, we have pursued the possibility of reacting SiH_4 with NH_3 at elevated temperatures. This reaction process has been studied extensively in vapor deposition of Si_3N_4 thin films for electronics⁽²²⁾ and formation of both amorphous and crystalline products were described.

2. Experimental

The starting materials were silane (electronic grade with Union Carbide Corp.), anhydrous ammonia (dried with Ca_3N_2) and purified argon.

The gases were metered into a fused silica reaction tube 3.8 cm diameter through flowmeters and separate concentric inlet tubes. The reaction tube was placed in a tube furnace and connected on the downstream end to a coaxial electrostatic separator operated between 5 and 15 kV and 0.2 to 0.5 mA. The outlet of the separator was terminated with a bubbler filled with an organic solvent which ensured positive pressure in the system. A liquid manometer indicated gas pressure in the tube.

The use of the electrostatic separator was essential because the reaction products formed a stable aerosol

(smoke) from which the solid could not be conveniently separated by other means. In the experiments, the furnace was heated to the selected temperature, the system purged with argon and the reactants were metered in. After termination of a run, the system was cooled to room temperature under flowing argon and disassembled. The reaction product was washed out of the tube and the separator by benzene.

The powder deposited predominantly downstream from the hot zone (60-70%) and a smaller amount was collected in the separator. In every run both portions of the product were recovered together. In the hot zone of the furnace an adherent CVD layer of Si_3N_4 always built up on the reaction tube. In about 4 to 5 hrs (duration of one run) a layer about 25 to 50 microns thick formed. The inner surface of the reaction tube was usually crazed after termination of every experiment, perhaps due to thermal expansion mismatch between the CVD layer and the fused silica glass. The CVD layer could be removed (flaked-off) from the tube by heating it to about 100°C above the reaction temperature.

In general, the product was a non-coherent powder and could be easily scraped out or washed out of the reaction tube. The recovered powders were either dried and stored in a nitrogen glove box or calcined in flowing ammonia directly after recovery from the reactor. The powders were characterized by X-ray diffraction, surface area measurements, electron diffraction and microscopy, and IR absorption spectroscopy. The reaction conditions for a number of experiments are listed in Table 2 and the characteristics of the powders are discussed below.

3. Results

The two main parameters which control the reaction between SiH_4 and NH_3 are temperature and ammonia-to-silane ratio. Below 500°C no appreciable reaction was observed and the gases ignited at the exit of the system due to the presence of unreacted and nonpyrolyzed SiH_4 . The only indication of a slight reaction was a light yellow, iridescent film which formed on the reaction tube wall.

With ammonia-to-silane ratios less than 10, (experiments 1-4, Table 2) brown to orange powders were obtained at temperatures between 700-900°C. The discoloration was presumably due to the presence of free silicon. This was supported by annealing experiments in nitrogen ($T > 1400^\circ\text{C}$) when these powders turned cream-white and gained weight (5 and 8% respectively for specimens 1

TABLE 2. REACTION CONDITIONS AND CHARACTERIZATION OF Si_3N_4
POWDERS SYNTHESIZED FROM SILANE AND AMMONIA

Run No.	Reaction Temp. °C	Flow Rates			Yield g	Product Color	Calcin. Temp. °C	Surface Area m^2g^{-1}
		Ar cm ³ /sec	NH ₃ cm ³ /sec	SiH ₄ cm ³ /sec				
1	820	4	12	3.2	18	light brown	-	26
2	780	4	12	3.2	14	brown	-	14
3	720	4	12	2	10	brown	-	15.5
4	920	4	12	1.2	15	light orange-brown	-	11.8
5	530	8	8	0.56	3	white	-	80
6	590	8	16	1.15	10	light tan	-	12.5
7	550	8	16	1.15	7	yellow	-	4.0
8-10	600	8	16	1.15	37	light tan	-	15
11-13	650	8	16	1.15	60	light tan	850 °C	7.9
14-15	750	4	16	1.15	35	white	1150 °C	10.5
16	850	4	16	1.15	15	light tan	1150 °C	-
17	850	4	30	1.15	15	light tan	1150 °C	14.4

and 2). The annealing of powder No. 3, which had the darkest color, brought about strong X-ray peak characteristics of silicon. The observation that annealing below 1400°C does not bring about much nitridation of the free silicon and that the brown color did not change after immersion in hot 15% KOH solution (which readily dissolves Si) suggest that the free silicon is in the form of particles coated with an impermeable layer of Si_3N_4 , which is not accessible to the reagent.

By increasing the ratio of ammonia/silane to greater than 10, white or light tan powders were obtained. The lowest temperature at which an appreciable yield was obtained was 530°C (No. 5). The yield increased with increasing temperature and was close to the theoretical value at and above 650°C. Further increase in the NH_3/SiH_4 ratio, beyond about 15, and in the reaction temperature, above 650°C, did not appear to have any marked effect on the appearance and yield of the product. Only a slight variation of color, white-to-cream, was noticed between separate runs; Nos. 8 through 17.

All the powders were amorphous to X-rays, including those calcined. Powders 1 and 2 were also found to be amorphous by electron diffraction. Most of these powders were amorphous up to $\sim 1480^\circ\text{C}$ at which temperature a 20 min anneal in N_2 brought about small peaks of $\alpha\text{-Si}_3\text{N}_4$ indicating poor crystallinity. This temperature agrees well with 1490°C found for crystallization of pure amorphous Si_3N_4 prepared by decomposition of silicon diimide to Morgan(21). The crystallization temperature of amorphous Si_3N_4 containing free silicon (No. 1-4) was substantially lower and proceeded between about 1250°C-1350°C and also yielded $\alpha\text{-Si}_3\text{N}_4$. It was generally found that the free silicon crystallized at temperatures approximately 50°C below the crystallization temperature for Si_3N_4 .

The crystallization temperature is related probably to stoichiometry of the amorphous product and is decreased by an excess of silicon. The amorphous-crystalline transition is usually sharp and strongly exothermic. Once initiated, the heat evolved accelerates the transformation process. This effect has been observed on amorphous powder compacts during heating-up. Near 1450°C the sample develops a hot spot which rapidly spreads over the specimen's surface and brightens the pellet for about two sec. In some instances, especially in the larger compacts, the sample would crumble.

The specific surface area of the prepared powders varied over a large range and did not seem to be related to the ammonia/silane ratios. Increasing temperature, however, clearly decreased the specific surface area of the product (Run No. 5-7 in Table 2). Other parameters; such as the distance of the gas inlet from the hot zone, also had an effect on the surface area, but were not investigated in the course of this study. The sample surface area, measured by low temperature nitrogen absorption, as a function of calcination temperature (30 min hold, nitrogen atm) for powder No. 11-13 is shown in Figure 5. Surface area decreases from 17 m^2/g at 850°C to 12.8 m^2/g at 1300°C and remains relatively unchanged up to about 1475°C.

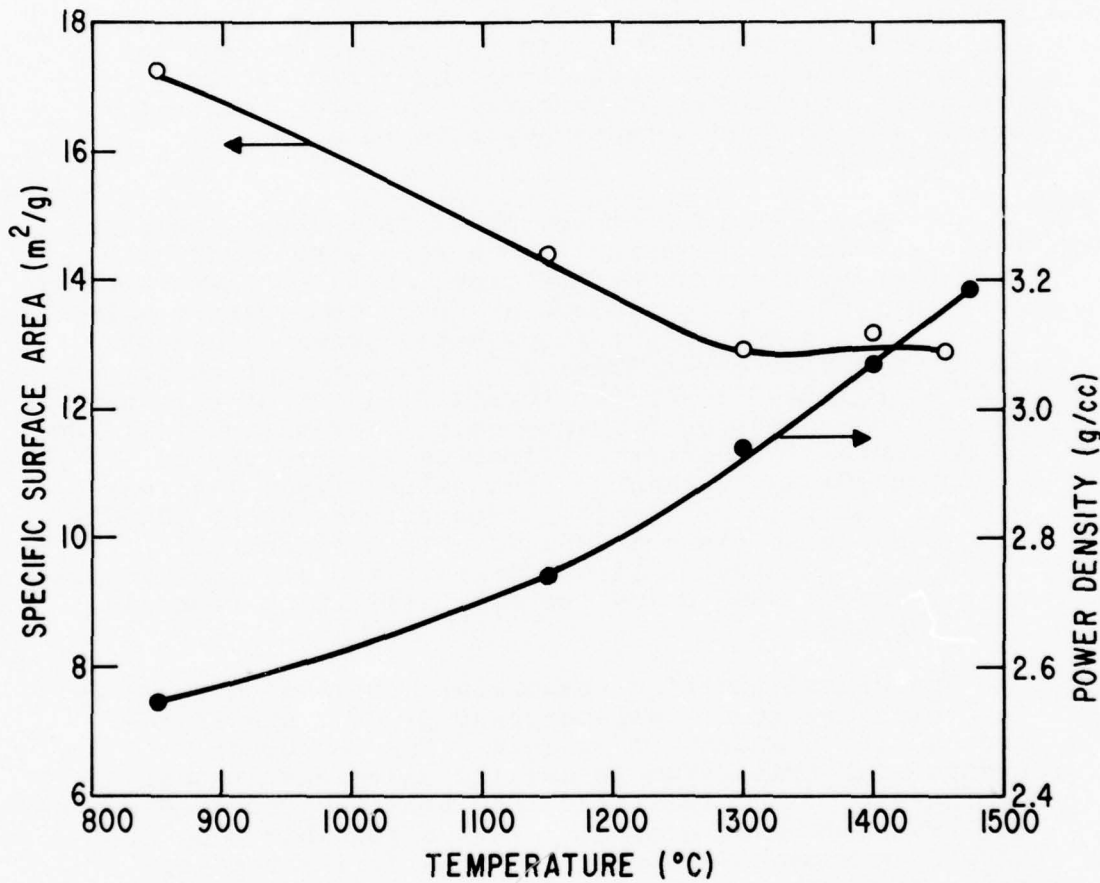


Figure 5. Surface Area and Density as a Function of Temperature for a Reaction Product of $\text{SiH}_4 + \text{NH}_3$

The same diagram shows also the change in density of the powder determined by helium displacement. There is a gradual increase in density from 2.55 g/cc at 850°C to ~3.18 g/cc (the theoretical value) at about 1475°C.

Measurements were not taken for powders prepared at temperatures below 850°C, however, still lower densities would be expected from the trend of the curve in Figure 5. A density of only 2.40 g/cc was reported for a product formed from $\text{SiH}_4 + \text{NH}_3$ by glow discharge at room temperature(23).

Gradual changes in the structure of the "as-prepared" silicon nitride as a function of temperature were followed conveniently by infrared spectroscopy. The absorption spectra of a series of powders obtained at different temperatures are shown in Figure 6(A-E). The absorption bands are identified in Table 3. It is observed that a low temperature product exhibits strong absorption bands characteristic for N-H and Si-H bonding in addition to the expected absorption due to the two basic Si-N stretching modes near 11.5 μ and 21 μ . In a sample prepared at 850°C (Figure 6(B)), the N-H and Si-H bands at 3.0 μ , 4.6 μ and 8.3 μ are substantially weaker but still well resolved, while after calcination at 1150°C there is only a slight trace of the N-H absorption near 3.0 μ . At this point, the identification of N-H absorption at 3 μ is uncertain due to the overlap with the weak O-H band near 2.8 μ , resulting from traces of water in the KBr used in the preparation of the specimen.

The absorption band, due to the symmetrical stretching of Si-N-Si at 21 μ , is very weak (and shifted) for the low temperature product and gradually strengthens as the reaction temperature increases, indicating an increase of in-line Si-N-Si bonding. The splitting of the Si-N bands due to crystallization of $\alpha\text{-Si}_3\text{N}_4$ is shown in the spectra in Figure 6(D-E). This reflects absorption due to modes resulting from the different N sites in the $\alpha\text{-Si}_3\text{N}_4$ lattice. Figure 6(D) shows a poorly crystallized powder, calcined at 1475°C, in which $\alpha\text{-Si}_3\text{N}_4$ lines were just about detectable by X-rays. In Figure 6(E) the spectrum of a well crystallized $\alpha\text{-Si}_3\text{N}_4$ is shown. This specimen was calcined at about 1350°C, and as mentioned above, its crystallization was enhanced due to the presence of free silicon.

The onset of crystallization can also be detected by transmission electron microscopy (TEM). A TEM micrograph in Figure 7 illustrates the typical morphology of particles of an amorphous Si_3N_4 powder. The spherical particles range in size between 0.03 to 0.2 μ and tend

BEST AVAILABLE COPY

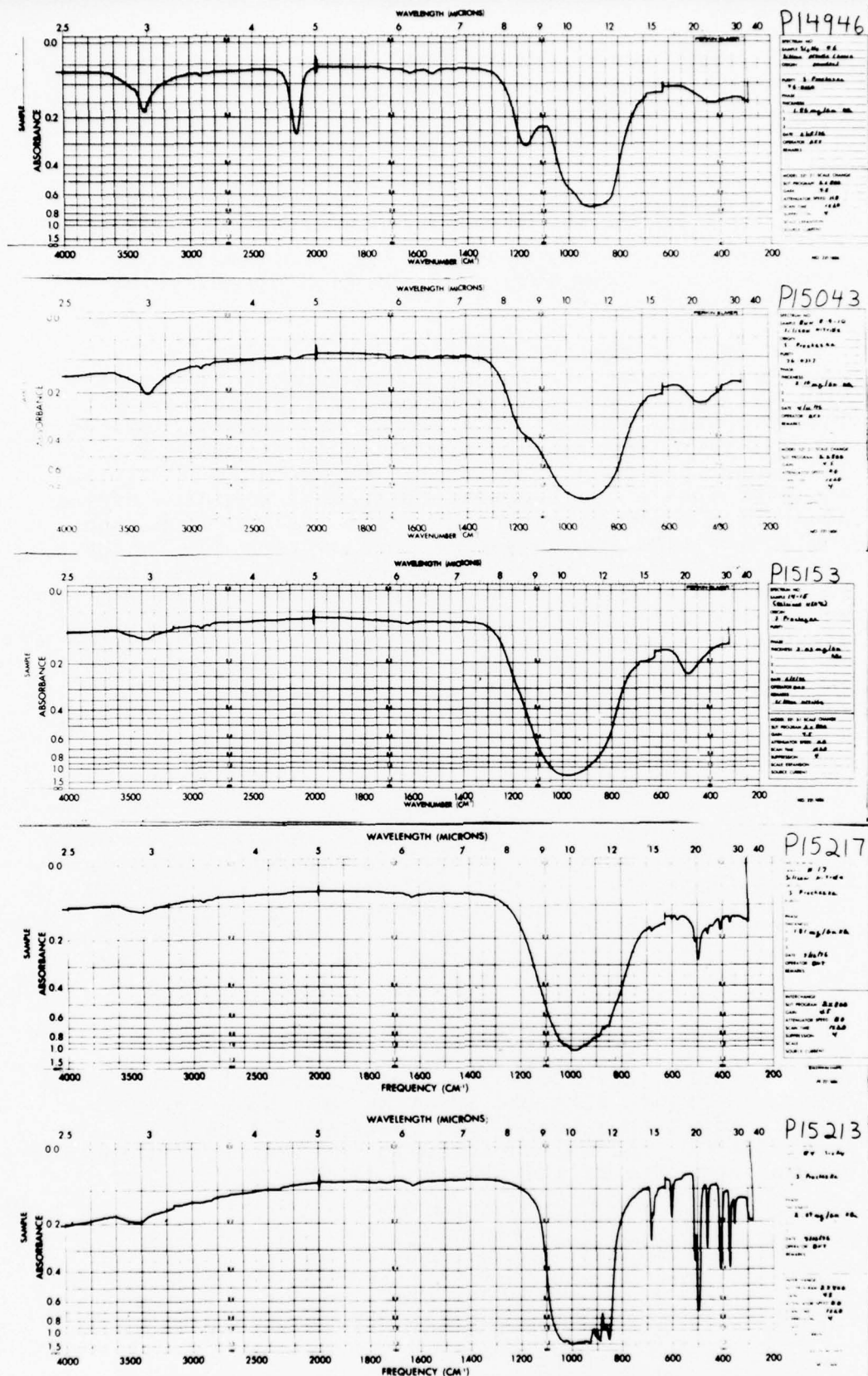


TABLE 3. I.R. ABSORPTION BANDS IN Si_3N_4
PREPARED AT VARIOUS TEMPERATURES

Prep. Temp. $^{\circ}\text{C}$	3.0 μ N-H	4.6 μ Si-H	8.3 μ N-H	11.5 μ Si-N	21 μ Si-N
590	st	st	st	vst	w
850	w	vw	w	vst	m
1150	vw	--	--	vst	st
1350	--	--	--	vst	vst
1475	--	--	--	vst	vst

vst = Very Strong
 st = Strong
 m = Medium
 w = Weak
 vw = Very Weak

Figure 6. I.R. Absorption Spectra of Reaction Products of $\text{SiH}_4 + \text{NH}_3$ (A) Synthesized at 600°C , (B) Synthesized at 850°C , (C) Calcined at 1150°C , (D) Calcined at 1480°C , (E) Silicon Rich Product Calcined at 1350°C



Figure 7. Particle Morphology of Amorphous Si_3N_4 Synthesized at 850°C . 30,000 X, TEM

to aggregate into loose clusters and chains. Even at the highest resolution no long range atomic order is observed in these particles which were also non-crystalline by X-rays (Figure 8). Particles of a powder annealed at 1425° , composed of crystalline $\alpha\text{-Si}_3\text{N}_4$ + trace of Si by X-rays, show an internal structure, some indication of faceting, and fringes i.e., evidence of a crystalline substance. Crystallization occurs probably by nucleation and crystallite growth within individual amorphous Si_3N_4 particles, and therefore, the crystallite size is by all probability initially independent of the starting (amorphous)

particle size. Upon heat treatment above the crystallization temperature, however, the crystallite size will increase rapidly due to high temperature and consume the entire volume of the starting amorphous particle which is contracting due to an increase in its density (see Figure 5).

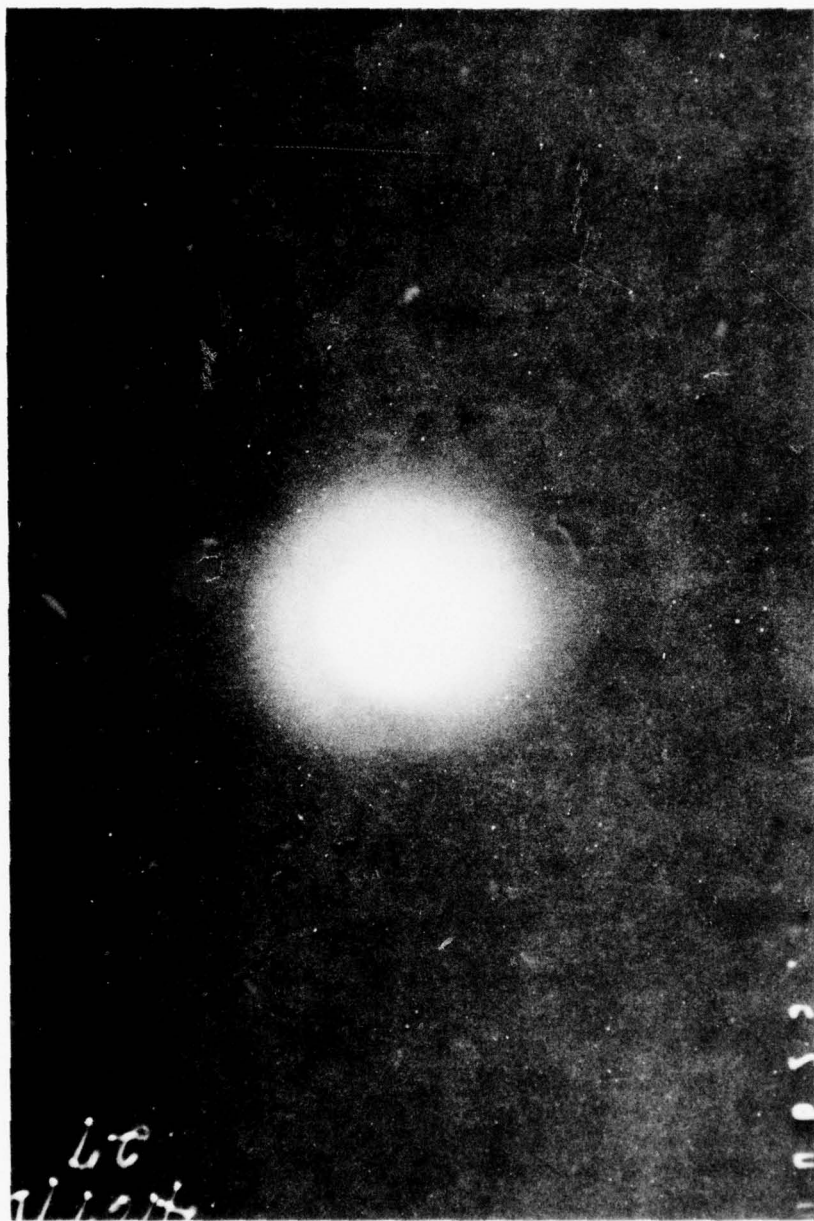
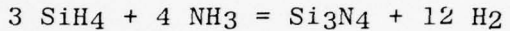


Figure 8. Electron Diffraction Pattern of Amorphous Si_3N_4

A detailed investigation of a silicon-rich powder calcined at a temperature slightly above the onset of crystallization revealed inclusions in some particles which could be identified by electron diffraction as silicon (Figure 9). Whether these silicon particles, which are generally less than 100 \AA in size, formed by precipitation during heat treatment from hyperstoichiometric silicon in the as-prepared, amorphous solid, or were formed by the initial decomposition of silane followed by Si_3N_4 formation, cannot be resolved at this time. However, judging from other observations (insolubility in KOH, formation of Si on SiH_4 pyrolysis) and other studies, both origins of silicon particles are possible.

4. Discussion

The overall reaction between silane and ammonia can be written:

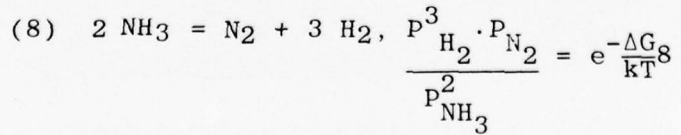
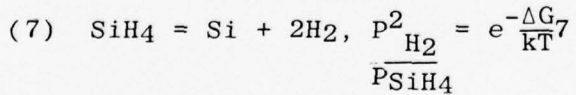


$$\Delta G_{800\text{OK}} = -6.7 \text{ MJ/kg} (-224 \text{ kcal/mole})$$

The probability for such a reaction to occur in one step would be negligibly small. Consequently, a series of successive reactions involving fewer molecules may be postulated:

- (1) $\text{SiH}_4 + \text{NH}_3 = \text{SiH}_3\cdot\text{NH}_2 + \text{H}_2$
- (2) $\text{SiH}_3\cdot\text{NH}_2 = \text{SiH}_2(\text{NH}) + \text{H}_2$
- (3) $\text{SiH}_2(\text{NH}) + \text{NH}_3 = \text{SiH}(\text{NH})\text{NH}_2 + \text{H}_2$
- (4) $\text{SiH}(\text{NH})\text{NH}_2 = \text{Si}(\text{NH})_2 + \text{H}_2$
- (5) $3 \text{ Si}(\text{NH})_2 = \text{Si}_3(\text{NH})_3 \text{N}_2 + \text{NH}_3$
- (6) $\text{Si}_3(\text{NH})_3 \text{N}_2 = \text{Si}_3\text{N}_4 + \text{NH}_3$

Two additionally important reactions are:



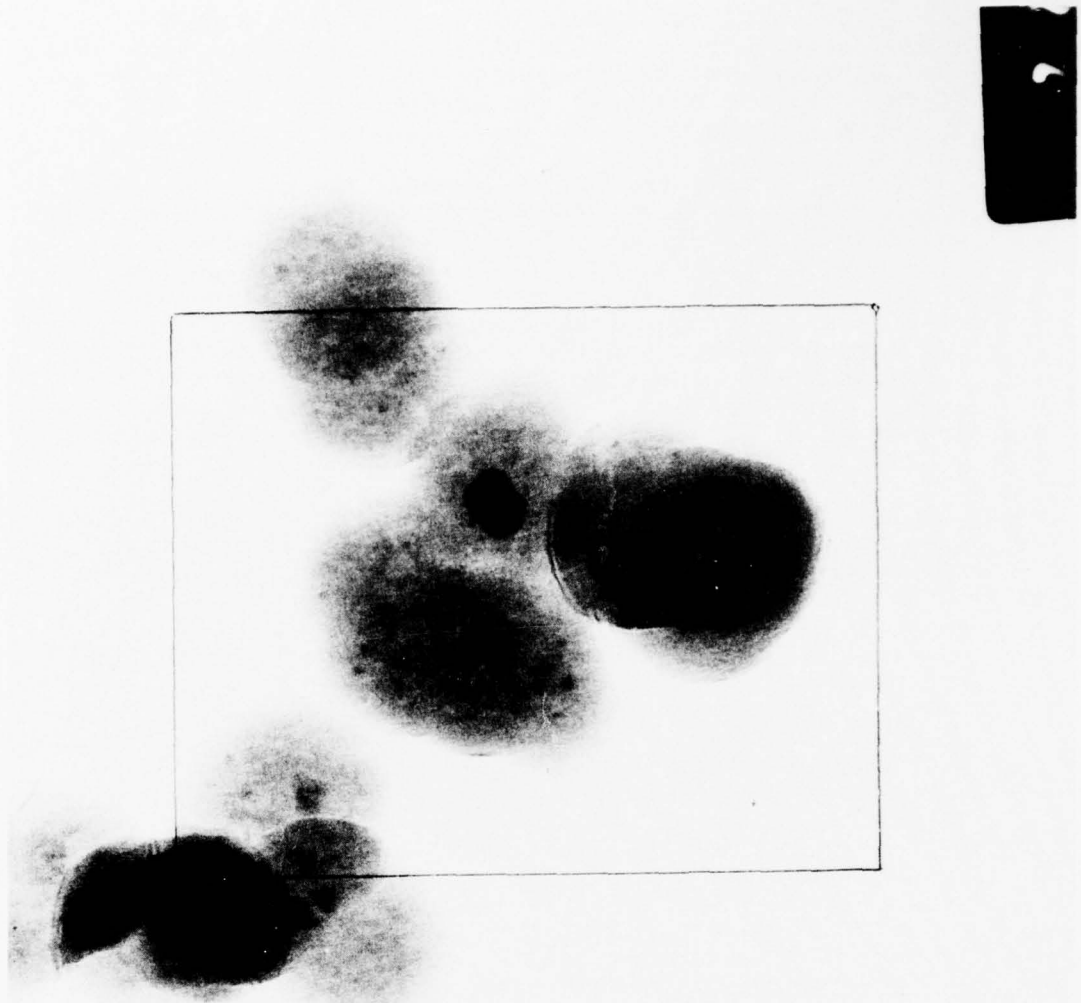


Figure 9. Elemental Silicon Inclusion in a Particle of Amorphous Si_3N_4 300,000 X, TEM

The sequence of reactions, (1-6), although purely speculative, helps to understand, at least qualitatively, the effect of ammonia to silane ratio on the formation of free silicon and also the origin of the N-H and Si-H bonds in the product.

As the temperature is increased, the partial pressure of hydrogen formed by reaction (8) controls the equilibria of reactions (1-4) and (7). Because of the quadratic dependence of its equilibrium constant on hydrogen pressure, the decomposition of silane into silicon and hydrogen (reaction 7) will be more suppressed by increasing P_{H_2} , and therefore, by the flow of NH_3 than any of the individual intermediate steps involved in nitride formation (reaction 1-4). Thus, a partial pressure of NH_3 and temperature may exist which retards or completely eliminates the formation of free silicon.

The presence of specific intermediates, as expected from the above reaction sequence, is probably unlikely. The best description of the product and its properties is obtained in terms of a three dimensional polymer, a concept suggested previously for amorphous CVD deposits.^(24,25) At low reaction temperatures both N-H and Si-H bonds are incorporated into the network and an open, random structure results. As the formation temperature increases, the atoms assume positions of closer packing and the relatively unstable bonds are removed, the less stable Si-H bond disappearing first. Depending on stoichiometry of the product, hydrogen and nitrogen will be given off and new Si-N or Si-Si bonds will form. Consequently the density of the solid increases. The product of reaction between SiH_4 and NH_3 will have rarely the stoichiometric ratio of silicon to nitrogen of 3:4. An excess of nitrogen, however, cannot be accommodated unless hydrogen is present and in such a composition so that the Si_3N_4 stoichiometry will be achieved on heating up to some temperature above 1100°C (by splitting of N_2 and H_2). A silicon rich network, on the other hand, when losing hydrogen, will readjust by forming Si-Si bonds or by reacting with some species from the environment, such as nitrogen, oxygen or water. Most likely both will occur, the former proceeding in the bulk and the latter at the particle surface.

The above picture of the structure of "amorphous Si_3N_4 " helps to explain a number of experimental observations and make some predictions:

1. The presence of Si-Si bonds will expand the structure due to the substantially larger covalent Si-Si bond lengths (2.3\AA) compared to that (1.6\AA) expected for the Si-N bond⁽²⁶⁾. Thus, a silicon rich amorphous Si_3N_4 will have

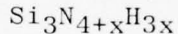
a more open structure, increased atomic mobility, and hence, a lower crystallization temperature.

2. A silicon rich amorphous Si_3N_4 will probably reject the excess silicon on crystallization because excess of silicon cannot be accommodated in the crystalline Si_3N_4 lattice. Thus, the appearance of crystalline silicon should approximately coincide with the crystallization temperature, as indeed observed.
3. The presence of Si-Si bonds is likely to bring about discoloration and decreased density of the amorphous Si_3N_4 .
4. The Si-H bond is unstable in the presence of H_2O , even at room temperature. A product containing these bonds will therefore tend to hydrolyze on exposure to ambient air, according to the reaction;



and consequently pick up oxygen. TGA results show that such powders heated in nitrogen or argon atmospheres (20 ppm oxygen) gain as much as 2.5 wt% at 400 to 500°C.

5. Nitrogen hyperstoichiometry (with respect to silicon) also occurs and is compensated by hydrogen atoms to obtain possibly,



Such compositions will yield stoichiometric silicon nitride upon heat treatment at elevated temperatures (1200°C). A small amount of hydrogen may be retained up to the crystallization temperature. TGA results on "as prepared" powders fired in a 10% H_2 -90% Ar atmosphere show a high weight loss, 5% at 500°C, which confirms the postulation of the presence of nitrogen hyperstoichiometry.

5. Summary

The synthesis of Si_3N_4 from SiH_4 and NH_3 is well understood and is a simple and practical process for preparation of laboratory quantities of silicon nitride. If carried out properly, a very pure product, low in oxygen, may be obtained. Under most conditions, the product appears to be slightly hyperstoichiometric in silicon. The excess silicon is at least partly pre-

cipitated during Si_3N_4 crystallization near 1475°C and nitrided at the same time (if nitrogen is available). This process is certainly amenable to scaling up. However, there does not seem to be a fundamental advantage over processes using silicon halides as precursors, provided these have the necessary purity.

Condensation reaction products obtained at lower temperatures from reaction between SiH_4 and NH_3 contain Si-H and N-H bonds. It is the instability of the Si-H bond, in contact with oxygen or water, which causes oxygen pick up in such a product. Powder synthesized or calcined at 850°C or higher temperatures are stable. The density of the powder increases gradually as the reaction temperature increases and approaches the value for crystalline Si_3N_4 near 1475°C . Crystallization in nearly stoichiometric compositions occurs near 1475°C , and this temperature is decreased by silicon hyperstoichiometry.

SECTION V

HIGH PRESSURE, HOT PRESSING OF PURE Si_3N_4 POWDERS

A. Objective

Attempts to consolidate Si_3N_4 without sintering aids under hot pressing conditions have shown (see below) essentially no densification at all. This information confirmed earlier findings that little densification occurred in Si_3N_4 except in one case where very pure Si_3N_4 , derived from silicon diimide, densified to $\sim 90\%$ density at 1800°C and 4 MPa (6000 psi)(21). In general, the nondensified, hot pressed materials were friable, poorly bonded compacts, with relative densities $\sim 50\%$.

The absence of densification in Si_3N_4 , as well as in other covalently-bonded solids such as C, BN, AlN and SiC, is probably related to low atomic diffusivity of the rate limiting species. Recent self diffusion studies(27) gave an estimate of silicon diffusion in Si_3N_4 of $\sim 1.5 \times 10^{-17} \text{ m}^2/\text{sec}$ at 1400°C as compared to $\sim 2 \times 10^{-17} \text{ m}^2/\text{sec}$ for the extrapolated diffusivity of Si in SiC. The self diffusion coefficient of N in Si_3N_4 was not obtained, but extremely low nitrogen diffusivity is expected from recent experiments in our laboratory. It was observed that pure, fine ($10 \text{ m}^2/\text{g}$) Si_3N_4 powders containing ~ 10 wt% free silicon could not be fully nitrided at temperatures of 1475°C , i.e., temperatures well above the melting point (1420°C) of silicon. Other indirect evidence for the very low mobility of Si and N in Si_3N_4 was the virtual absence of creep in CVD Si_3N_4 at 1550°C as mentioned above(16).

The absence of bonding, i.e., interparticle contact growth in hot pressed samples is more difficult to account for. Si_3N_4 is known to have a relatively high vapor pressure, and hence, particle growth is expected, and is indeed observed on heat treatment of powder compacts. The same transport mechanism should bring about interparticle contact growth as is observed in other substances with relatively high vapor pressure, such as AlN , NaCl , MoO_3 , etc. Contrary to expectation, bonding in pure Si_3N_4 is, in most cases, poor. Hot-pressed Si_3N_4 powders can be scratched with a fingernail and crumbled between fingertips. On the other hand, Si_3N_4 formed *in situ* by nitridation of silicon seems to exhibit ample intergranular bond formation. This peculiar behavior of Si_3N_4 is inconsistent with the understanding of the physical processes involved in sintering and is obviously the key problem in the study directed towards developing a consolidation process for this material.

Consequently, to better understand intergranular bonding and determine the lower temperature limit at which densification (or atomic mobility) becomes appreciable, Si_3N_4 was consolidated under diamond forming conditions followed by heat treatment of the resulting compacts. Densification under diamond forming conditions would not be, however, a sufficient criterion for bonding and atomic mobility. Nadeau(28), who studied high pressure hot pressing of silicon carbide, has observed that with some powders, 95% of theoretical density could be obtained at 5 GPa (50 kb) and temperatures $< 1500^\circ\text{C}$ by rearrangement and fragmentation of grains, and that the resulting compacts had a dense ceramic appearance. However, such compacts could not be satisfactorily ground and polished, and showed very low microhardness values and specific microstructures. Therefore, microstructural studies, indentation hardness, and X-ray diffraction analyses were selected as the prime characterization methods. In addition, compacts were annealed at various temperatures to determine whether or not grain growth occurred. Grain growth in pure Si_3N_4 , if detected, would be sufficient evidence that sufficient atomic mobility exists to make consolidation by sintering processes possible, at least in principle.

B. Experimental

The apparatus and procedure for ultra-high pressure consolidation of Si_3N_4 powders has been essentially the same as used for diamond synthesis, and has been adequately discussed previously(29). The only necessary change has been the use of a boron nitride liner within the carbon heater to prevent Si_3N_4 -carbon interaction. The liner consisted of a thin-walled tube and bottom and top spacers, all of which were machined from commercial BN stock to fit into the carbon heater. Pellets 0.95 cm x 0.64 cm were prepressed from the powders, repressed isostatically at 200 MPa (30,000 psi) and

prefired in nitrogen or NH_3 at 1200°C . Two of these fired pellets would fit into the cell. Preliminary experiments showed that 1400°C was the lowest temperature that could be used to obtain good bonding and densities. Therefore, the present series of experiments was carried out in the region 1400 - 1600°C . Temperature was obtained from power readings and calibrations and was accurate within $\pm 50^\circ\text{C}$. The specimens were held at temperatures for 20 min under 5.5 GPa.

The high-pressure hot pressing experiments were carried out using fine Si_3N_4 powders. Powder 1 and 5 (Table 4) were prepared in our laboratory as described in the previous chapter. They had surface areas 26 and 14 m^2/g and oxygen contents of 0.5% and 2.0% respectively. No. 1 was silicon rich. Powder 2 was a white amorphous material derived from ammonolysis of SiCl_4 with surface area of 43 m^2/g and an undetermined amount of oxygen. Powder 3 was Sylvania SN-502 described in section III, surface area 4.5 m^2/g and $\approx 1\%$ oxygen. Powder 4 was the SN-502 powder processed by vibratory milling for 6 hrs with cemented tungsten carbide balls in a plastic jar in benzene. The tungsten carbide pickup corresponded to less than 1 wt% W.

The pills obtained after compaction are about 0.6×0.3 cm in size and are rarely free of cracks. Usually severe cracking occurs on pressure relaxation due to differences in compressibility of the cell components. The typical appearance of a specimen crosssection is shown in Figure 10. After recovery, the specimens were boiled in concentrated HCl to remove residue of adherent BN. Density was determined by liquid displacement or by floating of specimen fragments in mixtures of $\text{CCl}_4 + \text{CH}_2\text{I}_2$ of known density. However, neither technique is accurate in this situation because of specimen cracking, and errors of ± 0.05 g/cc are anticipated. Also the cracks made it impossible to determine accurately whether the specimens had open porosity or not. Phase composition was determined by X-ray diffraction on a diffractometer. For metallography, specimens were mounted, ground and polished with 3μ diamond grit. No satisfactory etchant was found and almost every specimen responded differently to those tried. Three chemical etchants were tried on Si_3N_4 with limited and variable success: (a) a boiling solution of 5 cc HNO_3 (concentrated), 30 cc HF (50%) and 25 cc H_2O_2 (30%), (b) a boiling solution of 15 cc HF (50%), 45 cc HNO_3 (concentrated) and 45 cc acetic acid and, (c) a melt of KOH-NaOH at 280°C . Etchant (c) caused severe pitting at particular spots and no effect elsewhere. Etchants (a) and (b) revealed some grain boundaries only. The character of the grooves (spotty appearance) obtained with these etchants is similar to the character of grain boundaries which contain SiO_2 in hot-pressed SiC , and it is possible that similarly in the present case, the reagents attacked only segregated impurities.

TABLE 4. RESULTS OF HOT PRESSING OF Si_3N_4 AT 5 GPa

Spec. No.	Starting Powder ⁺	Pretreatment of the Pressings	Consolidation Temperature $^{\circ}\text{C} \pm 50$		Appearance	Density g/cc	Phases Present	Micro-hardness (Knoop) @ 200g load		Grain Size Estim. (μ)
			1500	1400				1100	-	
1	1	NH_3 , 1200°	1500		Dark gray, fragmented	2.75	n.d.	1100	-	<0.2
2	1	NH_3 , 1200°		1400	Dark gray	3.11	$\beta\text{-Si}_3\text{N}_4$ Si trace*	3080		<0.2
3	1	N_2 , 1200°	1600		Dark gray	3.05	$\beta\text{-Si}_3\text{N}_4$ Si trace*	3000		<0.2
4	2	NH_3 , 1200°	1500		White, fragmented	2.57	n.d.	n.d.	n.d.	n.d.
5	2	NH_3 , 1300°		1550	White, cracked	2.90	$\beta\text{-Si}_3\text{N}_4$	250		bimodal 0.2 \pm 0.8
6	3	N_2 , 1200°	1500		Ivory, cracked	2.65	n.d.	n.d.	n.d.	n.d.
7	3	N_2 , 1200°	1550		Ivory, cracked	2.89	$\alpha\text{-Si}_3\text{N}_4$ <10% β	1200	<0.5	
8	4	N_2 , 1200°	1500		Gray, cracked	3.15	$-\text{Si}_3\text{N}_4$	2500	>1	
9	4	N_2 , 1200°	1550		Gray, cracked	3.19	n.d.	n.d.	n.d.	
10	5	N_2 , 1200°	1550		Gray, cracked	3.15	$\beta\text{-Si}_3\text{N}_4$	n.d.	n.d.	

^{*}Less than 5%⁺See text for identification



Figure 10. Section of a Typical Si_3N_4 Specimen
Compacted at 5 GPa and 1500°C

The difficulties with etching and the very limited amounts of experimental material made grain size measurements uncertain. Nevertheless, by combining TEM (double stage replicas), optical microscopy and SEM fractography estimates of grain size could be made and are reported in Table 4.

Annealing experiments were done by packing the pills into Si_3N_4 powder in a small BN crucible and heating in a

carbon resistance furnace in nitrogen at about 1650°C, 1750°C and 1850°C for 40 min. However, none of the specimens survived 1850°C without serious degradation.

C. Results

In the following, the response of each of the Si_3N_4 powders and the characterization of the resulting microstructure are discussed separately. Some of the results are summarized in Table 4.

Figures 11 and 12 give TEM of replicas of a fracture surface and of a polished and etched surface of specimen 2. This specimen contained grains of free silicon which were revealed as a result of etching (rounded white spots, Figure 12). The silicon phase in this specimen does not tend to distribute itself along grain boundaries, but forms discrete grains. Their rounded shape suggests that a ratio of the grain boundary energy of Si_3N_4 to the $\text{Si}-\text{Si}_3\text{N}_4$ interfacial energy is close to 1.

Very few pores can be seen, which confirms the high density value measured (3.11 g/cc). The grain size was estimated from Figure 12 to be near 0.2 microns, which is about the maximum particle size of the starting powder, implying that little grain growth occurred during the high pressure consolidation. On the other hand, interparticle bonding is excellent, as shown by the Knoop indentations (200 g). The value of 3080 found, is in fact, higher than those previously reported for dense Si_3N_4 . Another interesting feature is the predominantly transgranular fracture in this specimen (Figure 11). Silicon nitride conventionally hot pressed with additives is known to fracture intergranularly.

Specimen 3 was annealed 40 min at 1650°C, 1760°C and 1850°C. No change in appearance or grain growth was detected by optical microscopy (2000 X) after exposure to 1760°C (Figure 13(A) and (B)). The specimen degraded on annealing at 1850°C as a result of crack growth due to evaporation, and was not evaluated metallographically.

Specimen 4 fragmented on removal from the pressing cell. This fragmentation could be partly suppressed by pretreating the precompacted pill at higher temperature, 1300°C, for 1 hr (Specimen 5). However, it is likely that particle coarsening occurred in this extremely fine starting powder at this temperature. Therefore, the grain size estimated from the micrograph on Figure 14 does not truly indicate growth during consolidation. Although about 90% of the theoretical density was achieved, bonding was poor as reflected by the low microhardness value. This suggests a case of a high degree of compaction achieved primarily by fragmentation and rearrangement under extreme pressure, similar to that

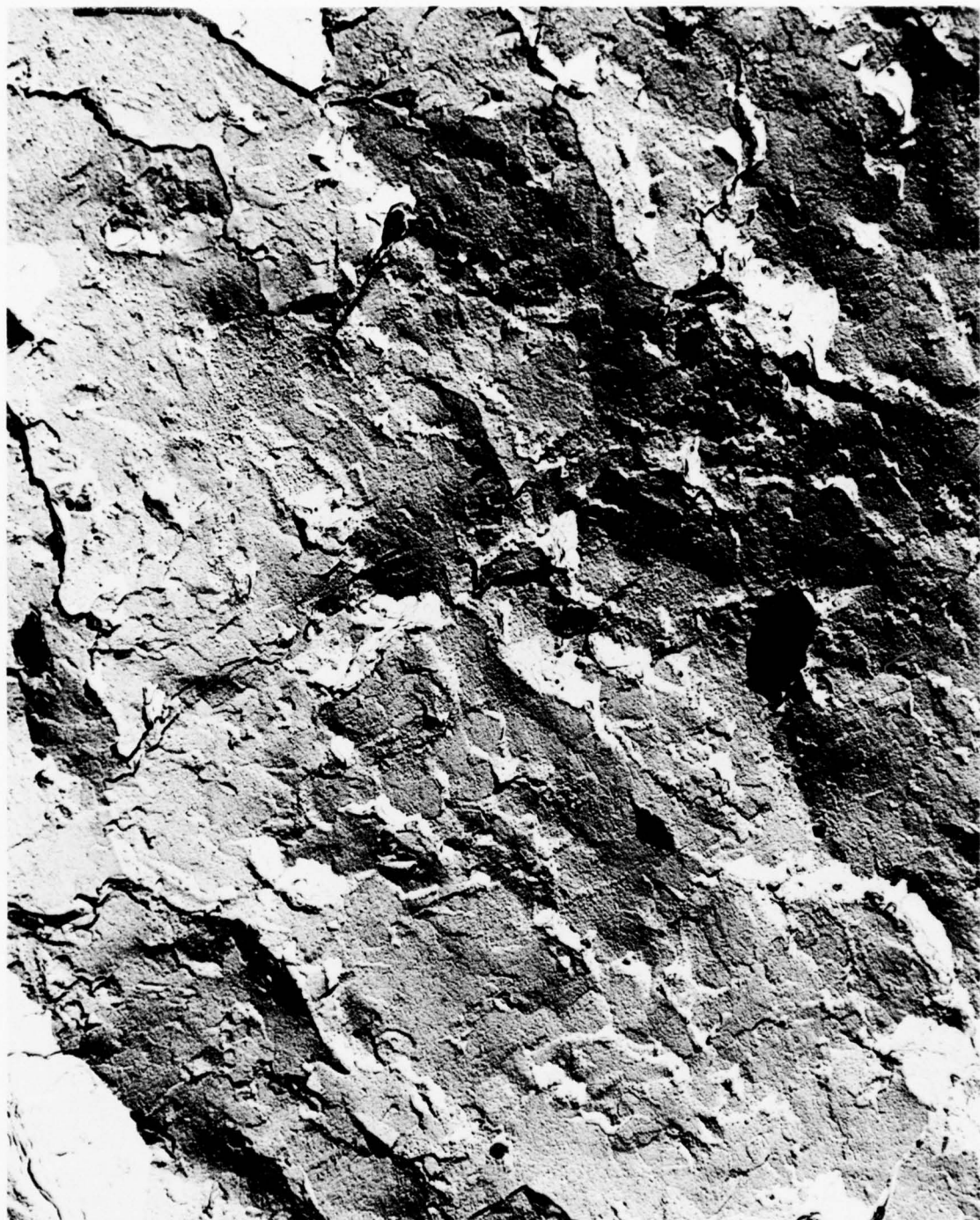


Figure 11. TEM of Replica of Fracture Surface of Si₃N₄
Compacted at 5 GPa at 1500°C. Specimen
No. 2 in Table 4. 30,000 X



Figure 12. TEM of Replica of Polished and Etched Surface of Specimen No. 2 White Spots Correspond to Leached Out Silicon Grains. 30,000 X

observed by Nadeau on SiC. In other words, the atomic mobility was very small in this Si_3N_4 sample at 1550°C .

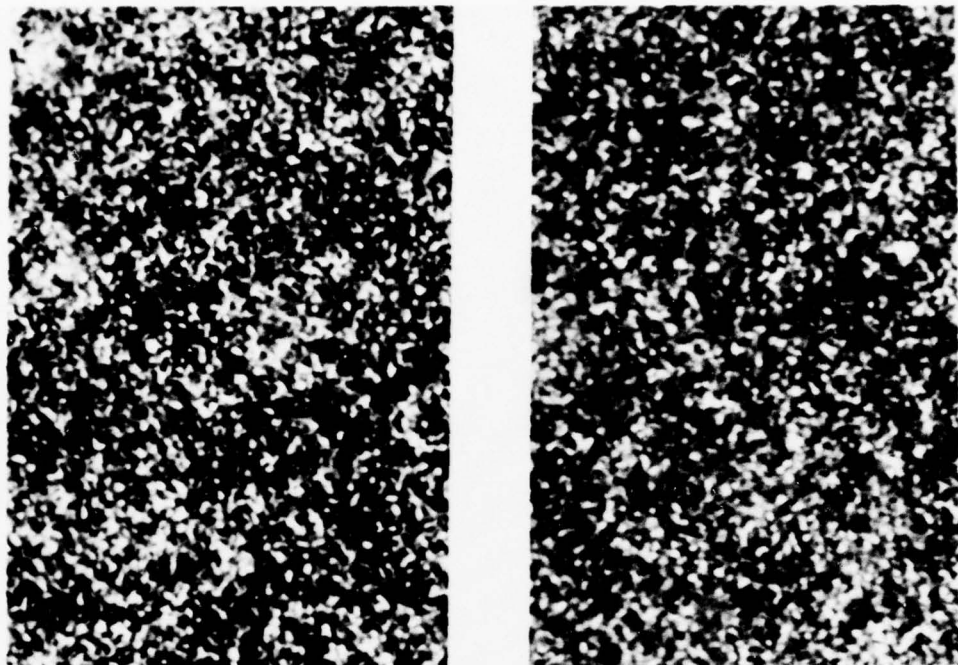


Figure 13. Hot-Pressed Si_3N_4 (A) As Polished, (B) Same Specimen After Annealing at 1760°C Hr 40 Min. Phase Contrast Micrographs, 2000 X

The fracture surface of specimen 7 is shown in Figure 15(A) and (B). This specimen was well bonded and had a relatively low microhardness, most likely related to the large volume fraction of round, nearly spherical pores. These round pores suggest that atomic mobility during the microstructure formation was appreciable. A crude estimate of grain size $\sim 0.5 \mu$ was made from the fractographs, because no information on grain size could be obtained on this specimen by polishing, etching, and replication for TEM. The etching treatments revealed only segments of some grain boundaries. It is speculated that the boundary pattern revealed by etching is due to segregated silica, i.e., only silica in grain boundaries was attacked by the etchant. This may be the case since no change in the pattern was observed by extended exposure to the etchant. In addition, a few sizable ($\sim 50 \mu$)

inhomogeneities having a much lower reflectivity than Si_3N_4 were observed in the as-polished surface of this specimen and were found to contain only silicon by the electron microprobe. This strongly suggests that the particles are SiO_2 .



Figure 14. Microstructure of Poorly Bonded, Hot-Pressed Si_3N_4 (Specimen 5) TEM, Double Stage Replica 30,000 X

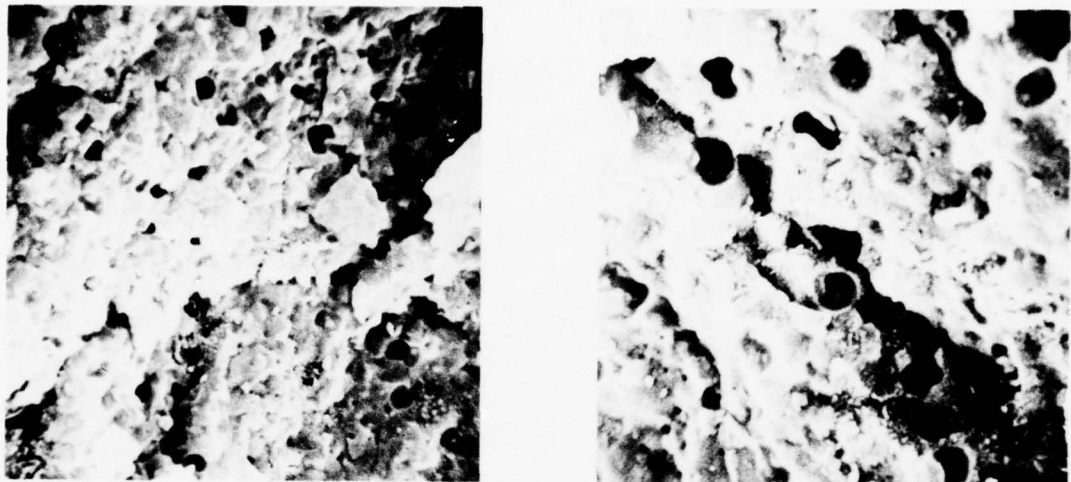


Figure 15. Si_3N_4 (SN-502) Hot-Pressed at 1550°C and 5 GPa.
SEM of Fracture Surface, (A) 5000 X (B) 10,000 X

The annealing of this specimen at 1650°C led to expansion and delamination, as shown in Figure 16. This resulted from the opening of numerous cracks perpendicular to the pressing direction and not from separation of individual grains, as shown in Figure 17. This photograph also shows that very little grain growth occurred.

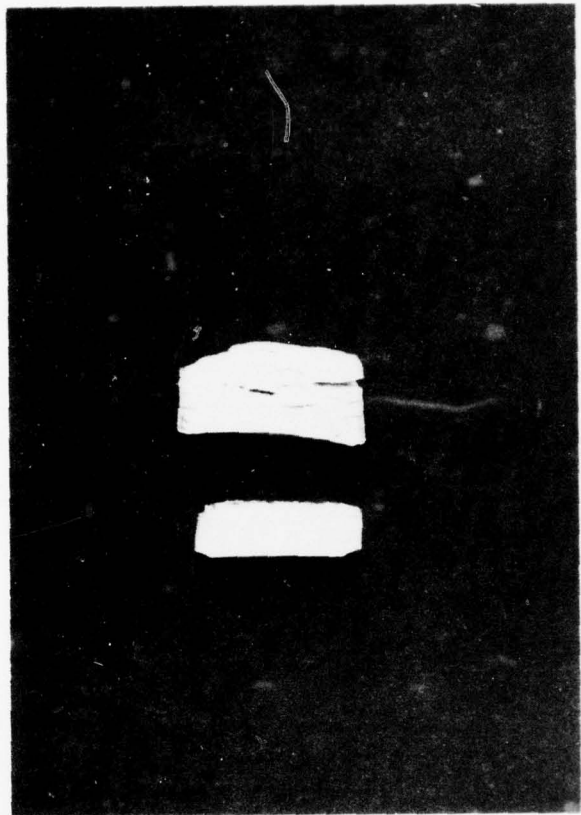


Figure 16. Piece of Specimen 7 (Table 4) Before and After Annealing (Upper Specimen) at 1650°C, 6 X

The processed SN-502 powder 4 gave rise to specimens 8 and 9 with the highest densities by high pressure, hot pressing. These specimens were well bonded together and exhibited a microhardness value of 2500. Very few small pores could be observed in the fracture surface of this specimen.

Specimen 8 was the only one which was composed of α - Si_3N_4 . All other specimens were β - Si_3N_4 only. There was considerable difficulty in obtaining a good grain boundary etch, so little information on grain size could be obtained. Nevertheless, the replicas (see Figure 18(A) and (B)) together with results of SEM seem to indicate that substantial grain growth occurred on annealing the specimen at 1750°C. It should be pointed out that there was no expansion or "bloating" of this sample during high temperature annealing. Thus, it appears that the processing of the powder with cemented carbide balls dramatically changed the microstructure and its high temperature behavior.



Figure 17. Surface of Annealed Specimen 7

Specimen No. 10 was hot-pressed from one of the later Si_3N_4 powders prepared in the laboratory (# 11-13, Table 2), much lower in free silicon than the powder used for specimen #1 and #2. The density was 3.15 g/cc. Sectioning revealed white islets about 100-300 microns in size associated with very fine pores ($\approx 1 \mu$) and a nonporous, brown matrix containing a few highly translucent areas. The inhomogeneity was almost certainly related to varying contents of free silicon in the starting powder. As only small amounts were available, the powder could not be effectively homogenized. Therefore, no detailed investigation of this pressing was done.

D. Summary

The important information obtained from the study of Si_3N_4 compacted under diamond forming conditions can be summarized into the following observations:

1. A temperature between 1500-1550°C is necessary to obtain good bonding in Si_3N_4 under compaction pressure of 5 GPa. The highest density, 3.19 g/cc, and microhardness, 3080 knoop/200g load, are in the range expected for a fully dense material.
2. Annealing the pressed compacts up to 1750°C produced little grain growth. The possible exception was one compact obtained from a powder milled with cemented carbide balls.

3. All the compacts showed inhomogeneities related to the presence of either SiO_2 or Si in the starting powders. Compacts which did not contain free silicon were white.
4. Pressure seems to enhance the α to β transformation in Si_3N_4 .

It was anticipated that a minimum temperature to obtain bonding in Si_3N_4 would be found from the high pressure, hot-pressing experiments. The results indicate that below about 1550°C there is not enough atomic mobility in "pure" Si_3N_4 to obtain sintering even under very high pressures. Therefore, densification cannot be expected at or below this temperature. By analogy to silicon carbide, which behaves similarly under diamond forming condition, one would predict that temperatures necessary for conventional hot pressing of Si_3N_4 to near theoretical density will be near 1800°C and for pressureless sintering near 2000°C , both estimated for relatively pure, submicron particle size starting materials (1850°C has been the lowest temperature at which boron doped SiC could be hot-pressed to >99% density, and 2080°C was necessary for sintering to terminal densities in excess of 95%).

SECTION VI

SINTERING BEHAVIOR OF PURE Si_3N_4

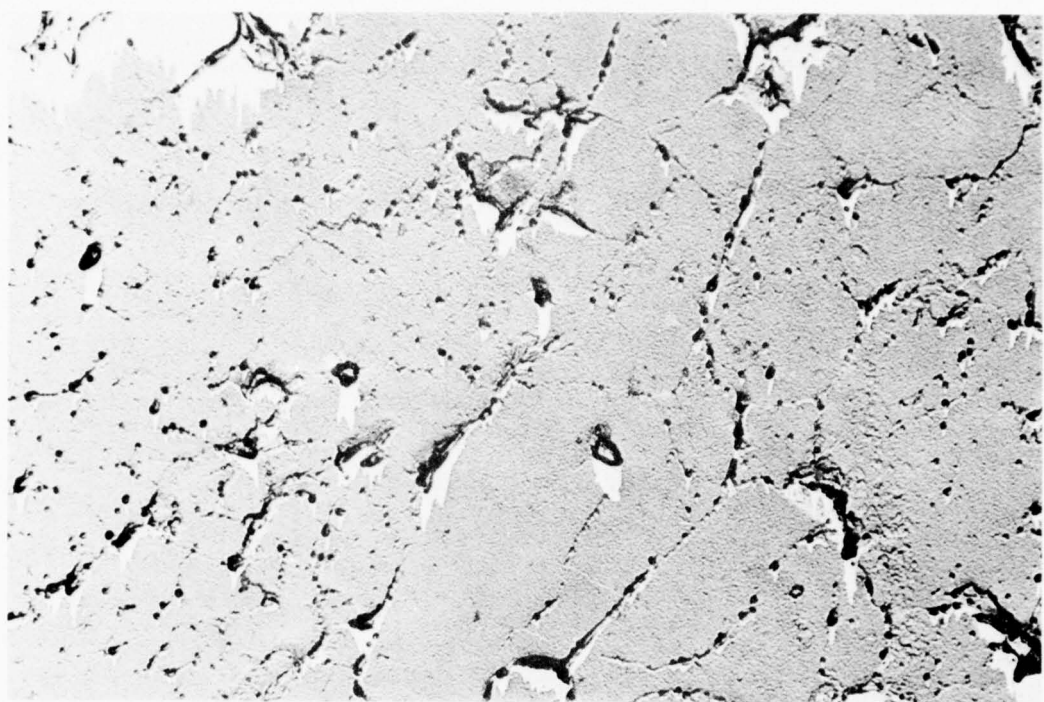
A. Introduction

The results of the high pressure, hot pressing of Si_3N_4 revealed that temperatures above $\sim 1550^\circ\text{C}$ would be required to promote sufficient atomic mobility for densification by sintering. On the other hand, thermal decomposition of Si_3N_4 will compete with sintering at high temperatures and may result in complex microstructures similar to those observed for β -SiC and Si_3 (¹⁶). Since no experimental data existed for weight loss, specific surface area and microstructural analysis of pure Si_3N_4 as a function of firing temperature, such an investigation was undertaken to further elucidate the sintering behavior of various Si_3N_4 powders at normal (0.1 MPa) and high (5-10 MPa) nitrogen pressures.

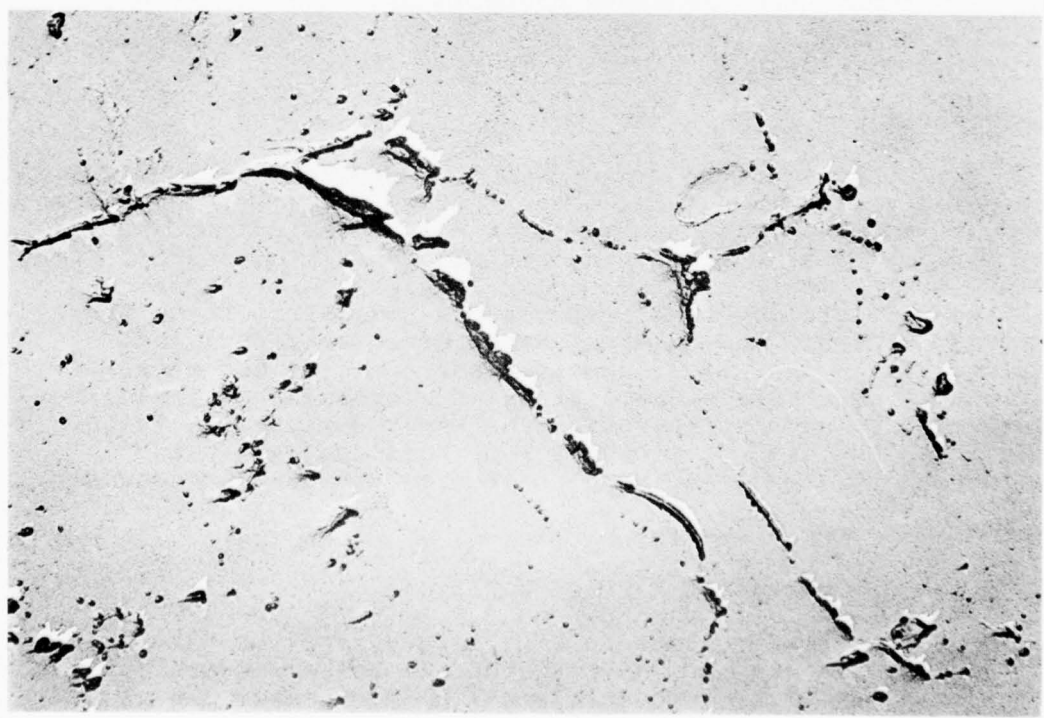
B. Normal Nitrogen Pressure

1. Powder Forming and Firing Conditions

Most powder compacts were formed from the "as-received" commercial and the "as-prepared" In House powders by die-pressing 1/2 g of powder in a 1.6 cm diameter die at 62 MPa and then isostatically pressing the resulting disc



A



B

at 200 MPa. The green density of SN-402 and In House Si_3N_4 compacts was ~35% of the theoretical value (3.18 g/cm³) and that of the SN-502 compacts was about 40%. Several of the heat treated powders which had lower oxygen contents were also fabricated into pellets in the same manner as described above.

Most of the firing experiments were performed in a programmable Mo-wound resistance furnace inside of which was located an Al_2O_3 tube, closed on one end. The Si_3N_4 compact was placed on a SiC setter which rested on an Al_2O_3 setter and the assembly pushed inside the Al_2O_3 tube into the hot zone of the furnace operating at 1000°C in one atmosphere of flowing nitrogen (15 cm³/sec). The thermal cycle treatment usually consisted of a heating rate of 4°C/min to the desired soak temperature, a soak time of 30 min and a cooling rate of 4°C/min down to 1000°C. Several powder compacts were fired to 1750°C under rapid heating rate conditions (~5°C/sec). A few samples were fired in a (N₂-5% H₂) gaseous mixture.

2. Characterization of Fired Si_3N_4 Compacts

The fired compacts were weighed and then measured for dimensional changes. Parts of the fired compact were (1) lightly crushed with a SiC mortar and pestle to make coarse powder for surface area measurements, (2) completely powdered for phase analysis by X-ray diffraction, and (3) fractured for the observation of microstructure by SEM. Occasionally, a whole sample was submitted for an oxygen analysis by neutron activation.

3. Results

The specific surface area and weight loss of compacts of SN-402 and SN-502 powders are shown as a function of temperature in Figures 19 and 20. In Figure 19 the Si_3N_4 (SN-402) compacts began to exhibit surface area reduction between 1200 and 1300°C and had the greatest surface area reduction between 1400 and 1600°C. The specific surface area after firing at 1400°C for 30 min in nitrogen is about 13.5 m²/g and at 1600°C is 1.6 m²/g. From 1600 to 1800°C the specific surface area changes very slowly from 1.6 m²/g to 0.8 m²/g.

Figure 18. Polished and Etched Surface of Specimen 8 (A) as Prepared at 1500°C (B) Annealed at 1750°C TEM, Double Stage Replica 24,000 X

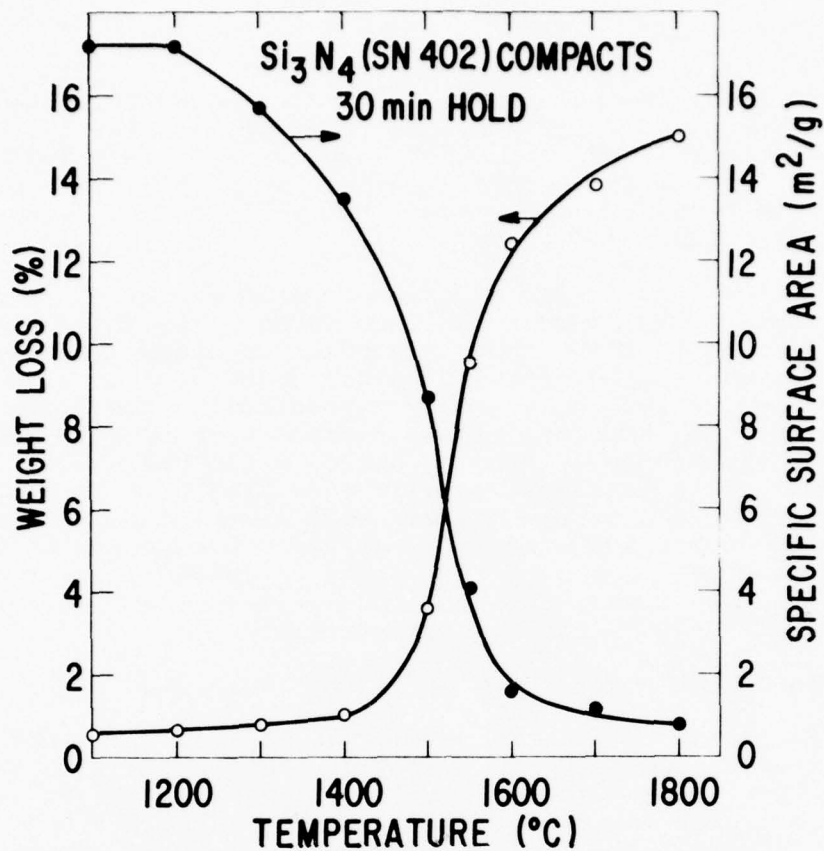


Figure 19. Weight Loss and Specific Surface Area as Function of Temp. for (SN-402) Si_3N_4 Compacts Fired for 30 Min in N_2

It should be pointed out that the apparent specific surface area of lumps of "green" compact of SN-402 powder was $15.5 \text{ m}^2/\text{g}$ as compared to $13 \text{ m}^2/\text{g}$ for the unpressed powder. In addition, compacts fired at 1100 and 1200°C had a specific surface area of $17.2 \text{ m}^2/\text{g}$ which is higher than that of the green compact. These differences are probably attributable to capillary condensation of nitrogen in the very fine ($<50 \text{ \AA}$) pores created in the green compact and in compacts fired at 1100 and 1200°C .

The weight loss data presented in Figure 19 show there is little ($<1\%$) weight loss up to 1400°C , a rapid increase in the weight loss between 1400 and 1600°C from about 1 to 12.5% , and a slow increase in weight loss from 12.5% at 1600°C to 15% at 1800°C . The weight loss of a compact prepared from vacuum-fired SN-402 powder containing 0.7 wt% oxygen was still very high, nearly 13% at 1700°C , indicating that most of the weight loss observed is independent of

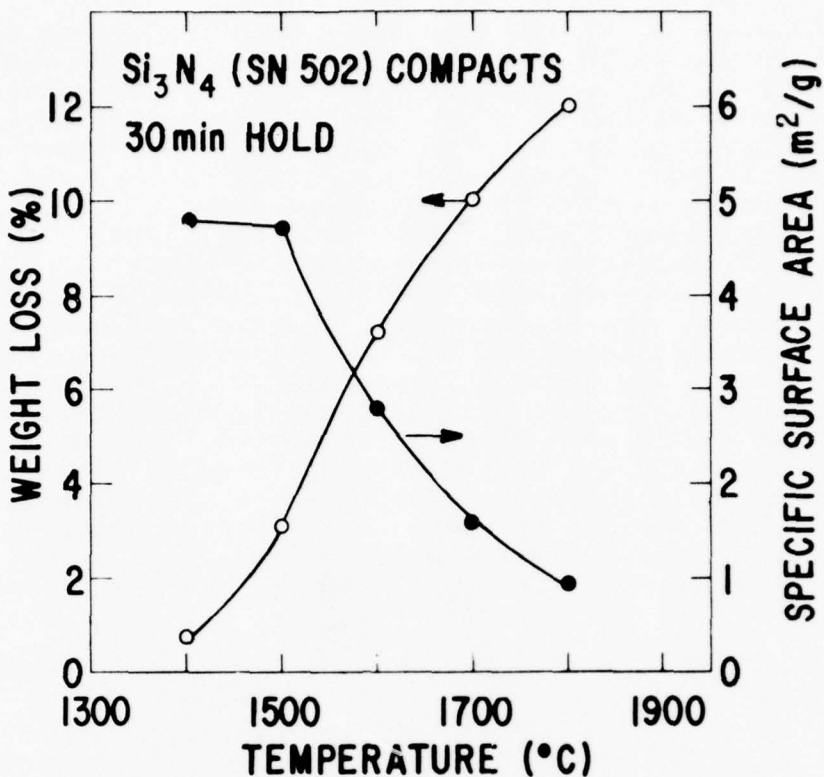


Figure 20. Weight Loss and Specific Surface Area as Function of Temp. for (SN-502) Si_3N_4 Compacts Fired for 30 Min in N_2

oxygen content of the starting powder. Finally, similar weight loss characteristics are observed for Si_3N_4 prepared by the reactions between $\text{SiCl}_4 + \text{NH}_3$ and $\text{SiH}_4 + \text{NH}_3$, which suggests that thermal decomposition is unaffected by chlorine impurities. The specific surface area and weight loss data as a function of temperature (Figure 20) for Si_3N_4 compacts made from SN-502 powder (94% α - Si_3N_4) also showed a major amount of weight loss in the same temperature region where a large reduction in specific surface area occurred. The specific surface area began to decrease at a much higher temperature ($\sim 1500^\circ\text{C}$) than that ($\sim 1250^\circ\text{C}$) observed for the SN-402 powder, which had a much higher, initial specific surface area. However, for the SN-502 specimens the beginning of weight loss occurred at the same temperature, $\sim 1450^\circ\text{C}$, as that observed for SN-402 specimens. The average weight loss for the SN-502 compacts fired at 1800°C was about 12% as compared to a value of 15% for the SN-402 compacts.

Fired compacts of the SN-402 and SN-502 starting powders did not undergo any shrinkage up to 1800°C and were weakly bonded together or crumbly. Microstructures of the fired compacts of SN-402 powder are presented in Figure 21 and show the fine grain-fine pore structure of a specimen fired at 1300°C (Figure 21(A)) as compared to the development of a large grain-large pore structure in a specimen fired at 1700°C. (Figure 21(B)). The "apparently" large ($\sim 2 \mu$) equiaxed grains observed (Figure 21(C)) are in fact dense regions composed of several faceted grains. The grains within a dense region appear to be well-bonded together, but there appears to be little bonding between the dense polycrystalline regions. Another interesting result was that the fired compacts were primarily composed of α -Si₃N₄ up to 1800°C. For example, compacts of SN-402 and SN-502 powders fired at 1800°C for 30 min in N₂ were composed of about 90% α +10% β -Si₃N₄ and 70% α +30% β -Si₃N₄, respectively, with no evidence of any free silicon or silica. However, free silicon was detected in a sample fired at 1750°C and quenched to room temperature.

Fired compacts of an amorphous Si₃N₄ powder (Run No. 3, Table 2), derived from the reaction between silane and ammonia (specific surface area of 15.5 m²/g), underwent about 9% and 12% linear shrinkage when fired in flowing N₂ at 1470°C and 1700°C, respectively. In both cases, however, the samples containing microcracks were very friable and did not exceed greater than 35% of the theoretical density. The color of the specimen fired at 1700°C turned from brown to light tan, indicating that a large fraction of the free silicon did nitride. Most of the shrinkage occurred in the amorphous state because the crystallization temperature for this powder was \sim 1490°C. In fact, linear shrinkage measured for a sample fired at 1510°C (i.e., the particles are now crystalline) was only about 10% as compared to 9% for the amorphous sample fired at 1470°C. These experiments proved that there is little effect of the amorphous-to-crystalline transformation on the sintering of Si₃N₄, and that the shrinkage observed is related to the increasing powder density of amorphous Si₃N₄ with increasing temperature (see Figure 5), accompanied by particle rearrangement in a highly porous (65%) compact. In addition, the microstructure of this fired compact was very similar to those represented in Figure 21.

4. Discussion

The observation that large weight losses (up to 18%) are accompanied by no change in the external dimensions of fired compacts due to actual sintering, strongly suggests that material loss occurs throughout the bulk



Figure 21. Scanning Electron Micrographs of Fractured Surfaces (SN-402) Compacts Fired 30 Min in N₂ at (A) 1300°C, (B) 1700°C and (C) 1700°C

of the porous (~65% porosity) sample. The similar weight loss of Si_3N_4 compacts made from starting powder containing 3.14 and 0.7 wt% oxygen and fired at 1800°C suggests that the major portion of material loss is caused by thermal decomposition of Si_3N_4 into Si and N_2 , and not by oxygen removal according to reactions described in Section IV-B. This suggestion is strengthened by the fact that a compact of (SN-402) Si_3N_4 powder fired at 1700°C for 30 min in nitrogen (10 ppm oxygen impurity) had a weight loss of 14% but still had an oxygen content of 1.8 wt%. Consequently, the maximum amount of weight loss expected from the oxygen removal reactions (Section IV-B) can only be about 6 wt%, based on the initial (3.14 wt%) and final oxygen contents of the Si_3N_4 . Finally, when a rapid heating rate of 5°C/min was used and the sample was quenched to room temperature, free silicon was detected by X-ray diffraction, suggesting that the proposed thermal decomposition reaction is valid.

The finding that large weight losses occur simultaneously with large reductions in specific surface area over the same temperature range (between 1400°C and 1800°C) in a nitrogen environment suggests that the weight loss of these compacts is sensitive to surface area and temperature. The sensitivity of weight loss to surface area is demonstrated by the experiment in which the resulting weight loss and specific area of an SN-402 compact fired at 1800°C for 30 min were ~15% and 0.8 m^2/g , respectively (see Figure 19), but upon refiring the same specimen for another 30 min at 1800°C in the same furnace, the resulting weight loss and specific surface area were only 0.7% and 0.7 m^2/g .

The large weight losses observed and the fact that a considerable amount of grain (particle) growth and pore growth takes place without any real macroscopic shrinkage lead to the conclusion that the sintering of pure Si_3N_4 powders having average particle sizes between 0.1 and 0.4 μ is prevented by high vapor transport and thermal decomposition. This deduction is, so far, based on the use of four relatively pure Si_3N_4 powders, three amorphous and one crystalline α - Si_3N_4 , derived from the reaction between SiCl_4 and NH_3 , and SiH_4 and NH_3 . If sintering is kinetically limited by a high ratio of matter transport by vapor phase transport as compared to volume and/or grain boundary transport, then a practical approach to densification of pure Si_3N_4 is to start with Si_3N_4 powder having an average particle size $<0.15\ \mu$ so that there will be a high probability for macroscopic shrinkage at temperatures at or below 1400°C, the temperature above which appreciable weight loss is detected (see Figures 19 and 20). However, the high temperature hot-pressing experiments showed that atomic mobility occurred

only at temperatures above 1550°C. The preparation of fine ($\leq 0.1 \mu$) Si_3N_4 powders and the introduction of additives may permit solid state sintering of Si_3N_4 (discussed below). If the thermal decomposition of Si_3N_4 is responsible for its nonsinterability, then both thermodynamic (surface energy) and kinetic considerations may be important. High nitrogen pressures (~5 MPa) would be expected to suppress the thermal decomposition of Si_3N_4 into Si and N_2 , and therefore, enhance the possibility of sintering. Experiments on this very topic have been carried out and will be discussed in the next section.

The weak "intergranular" bonding or crumbliness of Si_3N_4 compacts fired at temperatures above 1400°C raises several important questions. Since it is mandatory to have good intergranular bonding for solid state sintering, it becomes important to determine if it is possible to obtain strong intergranular bonding in pure Si_3N_4 . From the experimental results presented it appears that the poor intergranular bonding is related to thermal decomposition of Si_3N_4 and not impurities. This concept is supported by the observation that compacts fired below 1400°C were stronger than those fired above this temperature.

Another interesting point is that for the silicon tetrachloride derived powders investigated, α - Si_3N_4 remained stable at temperatures up to 1800°C, whereas Si_3N_4 powders derived by the reaction between SiH_4 and NH_3 converted almost entirely into elongated grains of β - Si_3N_4 at 1800°C in nitrogen. This evidence may suggest that impurities, perhaps chlorine, stabilize α - Si_3N_4 at very high temperatures.

C. Effect of High Nitrogen Pressures

A number of firing experiments were carried out on Si_3N_4 compacts at nitrogen pressures between 5 and 8 MPa (50-80 atm) to determine if the thermal decomposition of Si_3N_4 could be sufficiently suppressed to permit sintering. Temperatures above 1800°C were employed to enhance diffusional processes which may activate sintering. An oxygen partial pressure much lower than 1 Pa, which was used for the previous experiments in 0.1 MPa (1 atm) of flowing nitrogen, was employed in several experiments to minimize possible oxidation of Si_3N_4 . Such experiments were conducted in a water-cooled tungsten resistance furnace having a hot zone 8 cm long and 2.5 cm in diameter. Temperature was measured by optical pyrometry by sighting on the specimen surface. The gaseous mixture selected for use was 95% N_2 + 5% H_2 , having an oxygen content of about 2 ppm. This gas was pressurized and maintained at the desired total pressure during the experiment. Several Si_3N_4 compacts were fired under high nitrogen pressure in a pressurized SiC tube. Results are given in Table 5.

TABLE 5. RESULTS ON SINTERING Si_3N_4
UNDER HIGH NITROGEN PRESSURE

<u>Experiment No.</u>	<u>Temp. (°C)</u>	<u>Time (min)</u>	<u>P_{N_2} (MPa)</u>	<u>$\frac{\Delta L}{L_0} (\%)$</u>	<u>$\frac{\Delta W}{W_0} (\%)$</u>
1	1850	45	4.7	1-2	10
2	>2100	5	4.7	+	60
3	2000	20	8	10	20
4	2100	15	8	20	21

+Shrinkage could not be determined.

In the first experiment, a Si_3N_4 SN-402 compact was fired for 45 min at 1850°C in 4.7 MPa of nitrogen and 300 pPa (3×10^{-15} atm) of oxygen. The fired compact was crumbly and exhibited a linear shrinkage of about 1-2%, weight loss of 10%, and specific surface area of $1.1 \text{ m}^2/\text{g}$. The relative bulk density of the fired compact was 33% as compared to 36% for the green compact. X-ray diffraction analysis showed that the fired compact consisted of about 70 wt% α - Si_3N_4 and 30% β - Si_3N_4 . The weight loss of 10% for the compact fired at 1850°C in 4.7 MPa of nitrogen is about the same weight loss as that measured for a compact fired at 1550°C in 0.1 MPa (1 atm) of nitrogen. This weight loss may be due to the thermal decomposition of Si_3N_4 into silicon and nitrogen, but the subsequent loss of silicon does not proceed completely via pure silicon vapor. If so, tungsten silicides would have been expected to form in the tungsten heating element, because a low temperature eutectic exists in the W-Si system at 1392°C . This finding and the observation that a creamy white condensate containing Si and Cl (H, N and O cannot be detected by the solid state X-ray detector on the SEM) deposited in the cold sections of the furnace suggested that silicon-bearing molecules, such as Si_xNy , and/or Si-Cl-N-bearing molecules may also exist in the system. On the other hand, the weight loss of 10 wt% observed corresponds exactly with the weight loss expected by the removal of all of the initial oxygen impurity (3.14 wt%) by reaction 2 (Section IVB), the reaction between Si_3N_4 and SiO_2 to give SiO and N_2 . However, oxygen determination by neutron activation analysis showed the fired sample contains about 1.7 wt% oxygen and proves that a large portion of the material loss is indeed associated with thermal decomposition of Si_3N_4 . Neither reaction 2 nor the thermal decomposition reaction can, however, account for the Cl loss from the sample during firing.

The microstructure of the fired compact (Exp. 1) is shown in Figure 22. In Figure 22(A) the equiaxed solid regions have an average size of about 2μ and are composed of α - Si_3N_4 grains, while the elongated grains, about 1 to 2μ long and 0.2 to 0.3μ in diameter, are β - Si_3N_4 as determined by electron diffraction patterns. The polycrystalline α - Si_3N_4 regions shown in Figure 22(B) appear to be dense, and contain thermal grooves at the grain boundaries.

A second experiment using high nitrogen pressure was designed to reduce the weight loss of SN-402 Si_3N_4 by enclosing the compact inside a BN crucible with a screw lid. Again, the total pressure of the 95% N_2 + 5% H_2 mixture was ~ 5 MPa. Unfortunately, because of problems associated with temperature control, the temperature exceeded 2100°C for 5 min. Observation of the fired material and a measured weight loss $\sim 60\%$ indicated that complete decomposition of Si_3N_4 occurred. There was a mixture of black and white

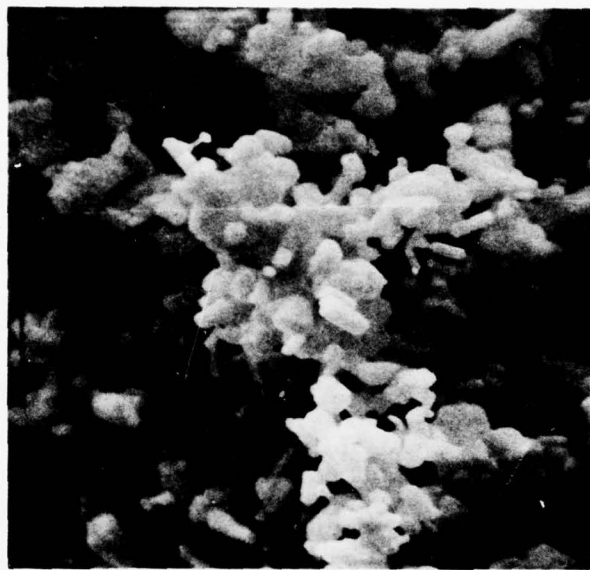


Figure 22(A). Scanning Electron Micrographs of Fractured Surfaces of (SN-402) Compact Fired at 1850°C for 45 Min in 4.7 MPa (47 atm) of N₂ 2500 X



Figure 22(B). Scanning Electron Micrographs of Fractured Surfaces of (SN-402) Compact Fired at 1850°C for 45 Min in 4.7 MPa (47 atm) of N₂ 10,000 X

material inside the BN crucible which was identified as silicon and β - Si_3N_4 , respectively, by X-ray diffraction. The silicon was present in the form of spherical particles, on many of which a layer of fine whiskers of β - Si_3N_4 grew. The β - Si_3N_4 phase is believed to have formed from the reaction between liquid silicon and high pressure nitrogen during cooling, because the large weight loss observed (~60%) is higher than that predicted (~40%) for complete decomposition of Si_3N_4 . The high weight loss observed was caused by diffusion of gaseous silicon out of the BN crucible and deposition on the cold surfaces of the furnace walls.

A reaction zone was observed on the tungsten heating element in the vicinity of the BN crucible. X-ray diffraction analysis showed the presence of WB, WB₂ and W in the reaction zone with no indication of any tungsten silicides, again indicating that the concentration of pure silicon vapor species is small in high nitrogen pressures. This reaction between BN and the tungsten heating element probably changed the electrical resistance of the heating element and was responsible for the difficulty in maintaining temperature control. As a result, BN does not appear to be a compatible crucible material for Si_3N_4 in tungsten furnaces at high temperatures.

Si_3N_4 powder #14 (Table 2), prepared from the reaction between SiH_4 and NH_3 , was compacted to a green density of ~32% and used for experiments 3 and 4 performed in the pressurized SiC tube. By using 8 MPa of nitrogen pressure and temperatures of 2000°C and 2100°C, the powder compacts shrank about 10 and 20% (linear), respectively, and exhibited about the same weight loss of ~20%. The sintered compacts were moderately strong, suggesting that significant bonding occurs between neighboring grains. A scanning electron micrograph (Figure 23) of a fractured surface of specimen 4 clearly reveals that the microstructure is composed of well bonded grains. Most of the grains are elongated and approximately 5-7 microns long and 2-3 microns wide. A small volume fraction of equiaxed grains can also be observed in Figure 23. X-ray diffraction analysis of this specimen showed only the presence of β - Si_3N_4 .

D. Summary

The thermal decomposition of Si_3N_4 can be suppressed and sintering enhanced at high temperatures by the use of high nitrogen pressures. The use of nitrogen pressures of ~8 MPa and temperatures between 2000°C and 2100°C permitted 10 to 20% linear shrinkage of compacts prepared from Si_3N_4 powder derived from the reaction between SiH_4 and NH_3 . Whether or not the sintering observed is characteristic of "pure" Si_3N_4 or is caused by impurity contamination from the SiC tube during firing is yet undetermined. By using



Figure 23. SEM Photomicrograph of Fractured Surface of Si_3N_4 Prepared in Table 1, Exp. No. 3
Mag = 2000 X

a nitrogen pressure ~ 5 MPa and low oxygen partial pressures ~ 100 pPa, a compact, prepared from Si_3N_4 powder derived from the reaction between $\text{SiCl}_4 + \text{NH}_3$, shrank only a few percent at 1850°C but had a weight loss ($\sim 10\%$) considerably lower than that ($\sim 25\%$) found when 0.1 MPa (1 atm) is used. Under the latter conditions, pore growth and grain growth occur in the absence of much macroscopic shrinkage, suggesting that vapor phase transport and/or thermal decomposition still dominate structural transformation(s) during firing. The relatively high weight losses of 10 to 20% at temperatures between 1850°C and 2100°C and at nitrogen pressures ~ 5 and 8 MPa tend to support this deduction.

Although some sintering takes place at temperatures between ~ 2000 and 2100°C , the highest final density obtained was only about 1.9 g/cc or 60% of the theoretical density of Si_3N_4 . Finally, the use of high nitrogen pressures appeared to enhance bonding between grains in the microstructure.

SECTION VII

HOT-PRESSING OF Si₃N₄ WITH ADDITIVES

A. Introduction

The inability to densify "pure" Si₃N₄ by sintering led to the investigation of the effect of chemical additives. The chemical additives selected were non-oxide substances. This restriction has been applied in an attempt to avoid formation of silicate melts and densification assisted by such liquids. Several nitrides and silicides were tried, as well as additions of elemental boron and carbon. The use of solute additives was desired, but in the absence of known phase equilibria and crystal chemical studies involving the solubility of small concentrations of dopants in the Si₃N₄ lattice, a semi-empirical approach was undertaken. This approach basically involved the selection of small atomic species which might substitute for Si or N in the Si₃N₄ lattice and enhance densification or sintering, perhaps by the formation of lattice defects and by decreasing the ratio of grain boundary energy to surface energy. This approach was previously successful for the sintering of β -SiC and Si⁽¹⁶⁾.

Hot pressing was used to determine the effectiveness of the additive. If the additive did not promote densification during hot pressing, then there would certainly be no possibility of densifying the same composition by sintering in the same temperature range. The hot-pressing temperature, 1750°C or 1800°C, was selected about 100°C below the thermal decomposition temperature for Si₃N₄.

B. Experimental

Powder compositions produced for hot pressing were prepared by mixing the desired weighed proportions of the chemical ingredients with a SiC mortar and pestle under benzene, followed by drying and collection. When hygroscopic chemical substances such as Be₃N₂ and Mg₃N₂ were used, all powder preparation procedures were carried out in a dry nitrogen glove box. Understandably, limited chemical homogeneity was expected by this mixing procedure. However, this was not a serious complication because only qualitative information was desired. Approximately 0.5 g of the resulting batch composition was loaded into a graphite die fitted with a 1 cm diameter BN insert. The faces of the graphite plungers were coated with a BN slurry before hot pressing.

The temperature and pressure cycle for a typical hot pressing run consisted of applying a pressure of 3.5 MPa at

room temperature and full pressure (55 MPa) at 1100°C. The time to reach 1750°C, for example, was about 15 min. After a soak time of 20 min in a nitrogen atmosphere at the hold temperature, the power to the induction coils was turned-off and the load removed. BN had to be removed from the resulting hot pressed sample before characterization. The cleaned hot pressed sample was then characterized, usually by X-ray diffraction, SEM, ceramography and displacement density.

C. Results and Discussion

The results for hot pressed, doped Si_3N_4 are shown in Table 4. Pure Si_3N_4 , SN-402 and Run 8-10 In-House powder, were densified to only 45 to 50% relative density at 1750°C for 20 min at 55 MPa. The addition of B in elemental form or in the form of BN had little effect on densification. Similarly, the simultaneous addition of small amounts of both B and C, additives which cause densification in SiC ⁽¹⁶⁾, did not enhance densification in Si_3N_4 . A typical SEM of a fractured surface of any of the B-doped, hot pressed samples showed that the grain size is very small or less than 0.1 μ . The specific surface area for the hot pressed sample of Si_3N_4 containing 3% B and 1% C was measured as $28\text{m}^2/\text{g}$, corresponding to an average spherical grain size of 0.07 μ . The lack of extensive macroscopic shrinkage combined with the suppression of grain growth and pore growth at 1750°C to 1800°C strongly suggested that under the experimental conditions employed, atomic mobility in Si_3N_4 containing C and/or B was very low. X-ray diffraction analyses on these hot pressed materials revealed little difference in the lattice parameters of α - Si_3N_4 with B and B+C additions. The measured lattice parameters for the α - Si_3N_4 phase in each sample were about $a=7.759\text{\AA}$ and $c=5.617\text{\AA} \pm 0.002\text{\AA}$, and it was impossible to detect a real change in the a - and c - values with composition. In addition, there did not seem to be major differences in the measured half-breadths of the X-ray lines, although "pure" Si_3N_4 had slightly sharper lines than any of the B- and (B+C)- doped Si_3N_4 samples.

The nonoxide additives that best promoted densification in Si_3N_4 were Be_3N_2 , Mg_2Si and Mg_3N_2 (Table 6). The relative density versus wt% Be_3N_2 in Si_3N_4 for constant hot-pressing conditions is illustrated in Figure 24. There is a maximum in relative density of about 98% between 1 and 2 wt% Be_3N_2 . The drop-off in relative density as the Be_3N_2 content increases beyond 2% is not yet understood but may be related to the formation of BeSiN_2 , which is detected by X-ray diffraction for compositions having >5 wt% Be_3N_2 . The Sylvania (SN-402) Si_3N_4 powder did not densify as much as the In-House Run 8-10 powder even though both powders were initially amorphous, of comparable specific surface areas, $\sim 10-13\text{m}^2/\text{g}$, and of the same oxygen content, ~ 3 wt%. A polished section of hot pressed (Run 8-10) Si_3N_4 doped with 1 wt% Be_3N_2 is shown

TABLE 6. RESULTS FOR HOT-PRESSED, DOPED Si_3N_4

Composition (wt %)	Hot Pressing Conditions	Rel. Density (%)	Phases Present		
			β (%)	α (%)	Other
SN402 Si_3N_4	1750°C-1200 sec - 55 MPa	45	10	90	
"	+ 1% B	46	20	80	
"	+ 4% B	46	20	80	
"	+ 1% BN	47	10	90	
"	+ 3% B+1%C	45	30	70	
"	+ 2% Be_3N_2	94	~100	"	
RUN 8-10 Si_3N_4	1750°C-1200 sec - 55 MPa	50	"	"	
"	+ 0.5% Be_3N_2	93	"	"	
"	+ 1% Be_3N_2	97	"	"	
"	+ 2% Be_3N_2	98	"	"	
"	+ 3.5% Be_3N_2	83	"	"	
"	+ 5% Be_3N_2	75	"	"	
"	+ 15% Be_3N_2	62	Major	"	
"	+ 0.5% Mg_2Si	74	60	40	
"	+ 1% Mg_2Si	86	60	40	
"	+ 2% Mg_2Si	100	30	70	
"	+ 3% Mg_2Si	100	70	30	
"	+ 5% Mg_2Si	100+	~100	tr.	
"	+ 10% Mg_2Si	100+	Major	tr.	
"	+ 2% Mg_3N_2	99	100	tr.	
"	+ 2% TiSi_2	65	60	40	
"	+ 2% MgO	96	80	20	

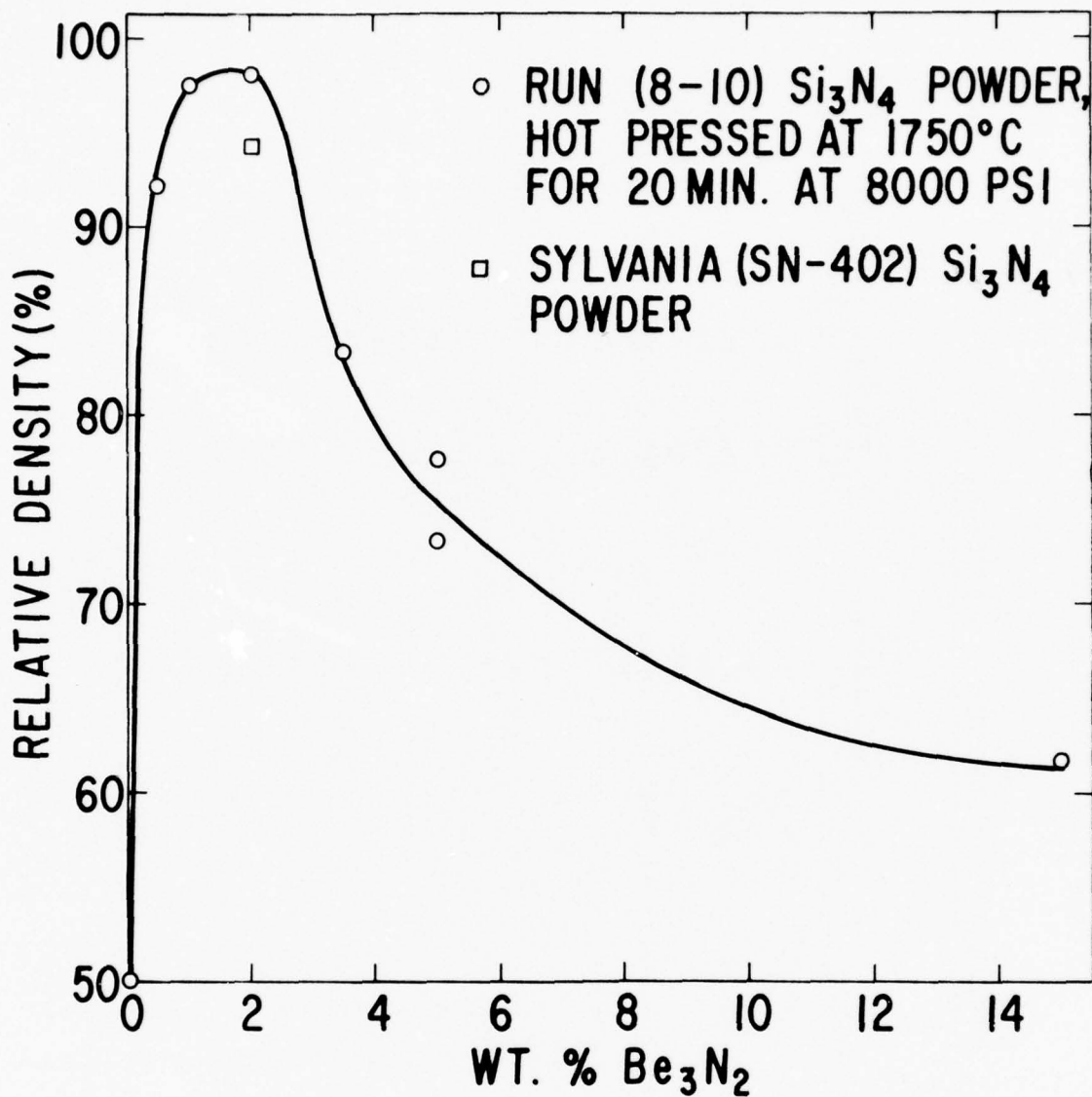


Figure 24. Relative Density of Hot-Pressed Si_3N_4 as Function of Be_3N_2 Content

in Figure 25. The dark spots are pores less than 4μ in size. The bright particles, although not positively identified, contain silicon and probably are silicon particles resulting from the presence of free silicon in the starting Si_3N_4 powder or from thermal decomposition during firing. Also, there appear to be dense regions elongated perpendicular to the hot pressing direction. The hot pressed samples were composed of nearly all β - Si_3N_4 . Chemical etching of the polished section was unsuccessful, and the same was true for other dense samples discussed below.

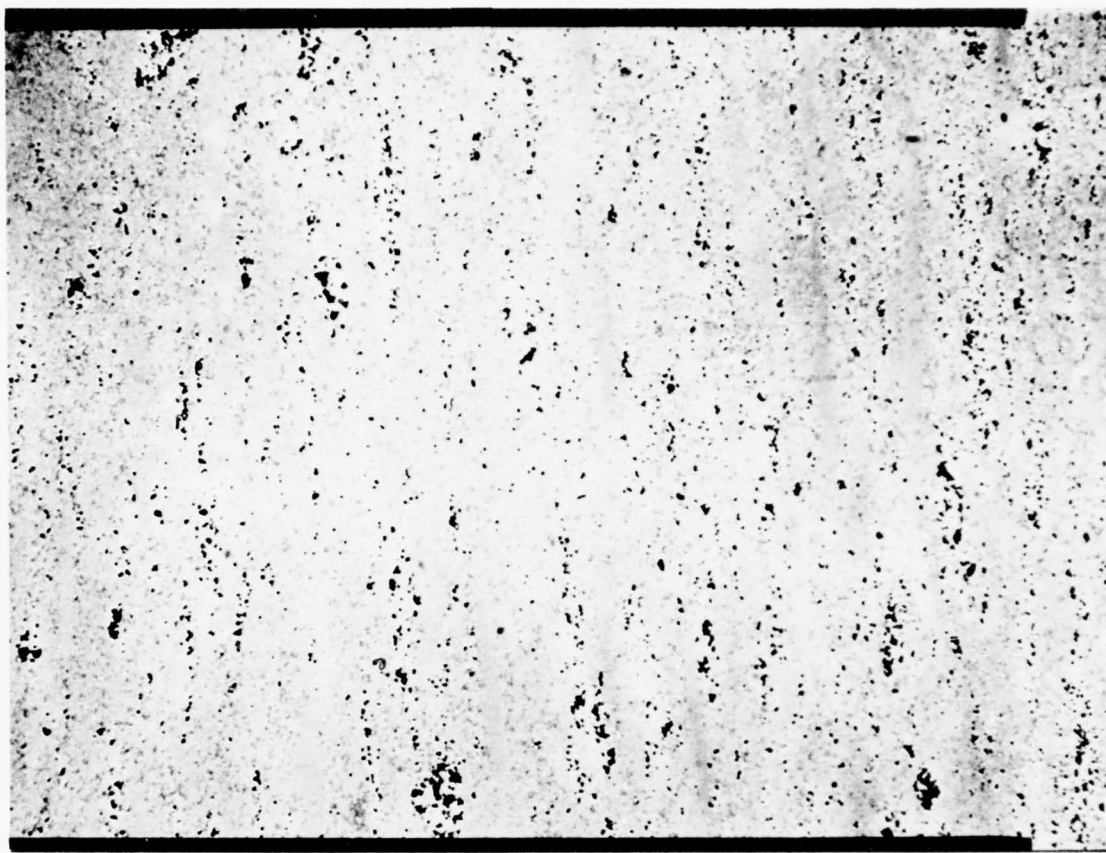


Figure 25. Reflected-Light Photomicrograph of a Polished Section of Hot-Pressed Si_3N_4 Doped with 1 wt% Be_3N_2 Mag = 500 X

The effect of Mg_2Si additions on the density of hot-pressed specimens is shown in Table 6 and Figure 26. Essentially full density is achieved by adding Mg_2Si in concentration ≥ 2 wt%. For compositions having ≥ 5 wt% Mg_2Si , an MgSiN_2 phase was detected by X-ray diffraction but had no apparent effect on final density. The microstructure of Si_3N_4 (Run 8-10) doped with 3 wt% Mg_2Si in Figure 27 shows (1) small islands of pores intermixed with bright particles, suggesting the pores may be a consequence of particle pull-outs, (2) small islands of bright particles which are probably free silicon, and (3) randomly dispersed bright particles. X-ray diffraction shows that the Si_3N_4 matrix is composed of $\sim 70\%$ β - Si_3N_4 and 30% α - Si_3N_4 .

The addition of 2 wt% Mg_3N_2 to Run 8-10 Si_3N_4 powder permitted the fabrication of 99% dense, hot pressed material composed of 70% β - and about 30% α - Si_3N_4 . The microstructure

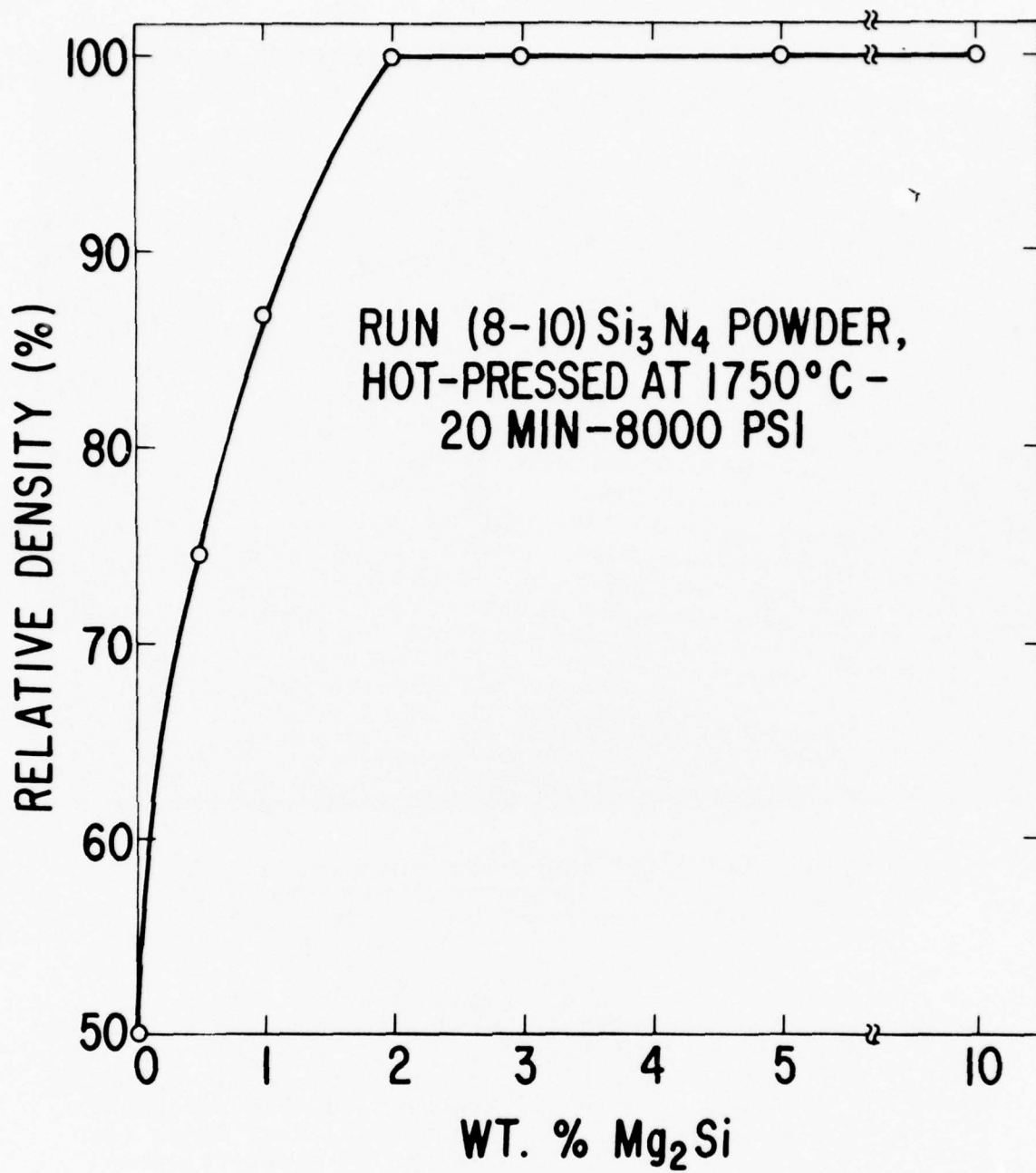


Figure 26. Relative Density of Hot-Pressed Si_3N_4 as Function of Mg_2Si Content

of this specimen, shown in Figure 28, is characterized by a small amount (1%) of micron-sized pores, and a relatively random distribution of bright particles, possible Si. No other features (Si_3N_4 grain size and shapes) could be observed in the polished section, even at magnifications up to 1000 X.



Figure 28. Microstructure of Hot-Pressed
 Si_3N_4 Doped with 2 wt% Mg_3N_2
 $T=1750^\circ\text{C}$, $t=20$ min, $p=8000$ psi

D. Summary

Silicon nitride can be densified to nearly full density by making additions of Be_3N_2 , Mg_2Si and Mg_3N_2 to high purity, submicron Si_3N_4 powders. If sintering and creep mechanisms are related, as frequently assumed, then the relatively high temperatures for the onset of densification ($\approx 1600^\circ\text{C}$) for Be_3N_2 - and Mg_2Si -doped Si_3N_4 of particle size $\approx 0.23 \mu$ may be a promising sign for good high temperature mechanical properties. Furthermore, failure of polished sections to etch in HF based etchants indicates that no major amount of silicate phase(s) formed.

The high temperature of 1600°C for the onset of densification in MgO -doped Si_3N_4 was unexpected. A characteristic temperature for the onset of densification was expected to be lower than 1500°C , according to the literature⁽³⁰⁾. Our

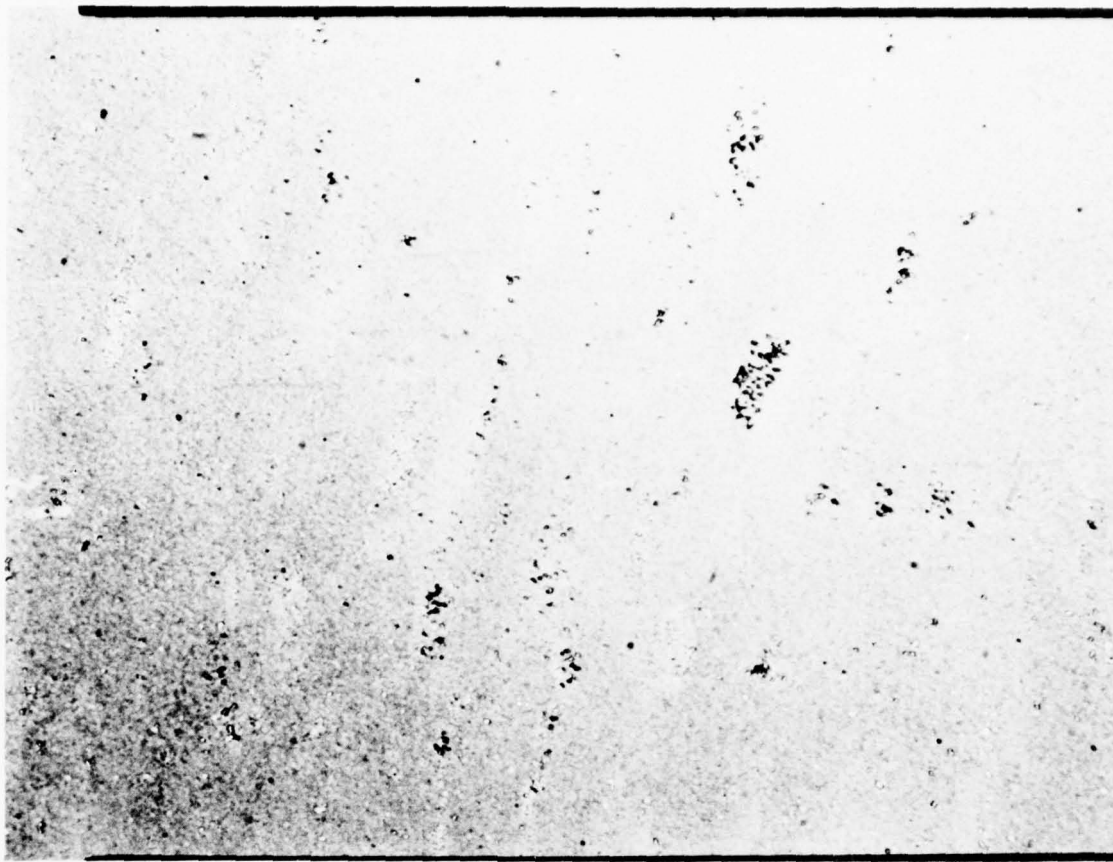


Figure 27. Microstructure of Hot-Pressed
Si₃N₄ Doped with 3 wt% Mg₂Si
Mag = 500 X

It was believed that the temperature for the onset of densification might be representative of some measure of the creep resistance of doped Si₃N₄. Table 7 shows the temperature for the onset of densification for pure and doped-Si₃N₄, which was taken to be that temperature at which the specimen densified to 55% of the theoretical value, since pure Si₃N₄ does not densify beyond 50%. In all cases, the hot pressing conditions were the same, i.e., constant heating rate (~20°C/sec) and an applied pressure of 55 MPa. Run 11-13 Si₃N₄ powder was used for all experiments. It had a specific surface area of 8 m²/g and an oxygen content of 1.94 wt%. The temperature for the onset of densification in pure Si₃N₄ is >1750°C. By doping with 2% Mg₃N₂, 2% Mg₂Si and 1% Be₃N₂, the characteristic temperatures for the beginning of densification are 1400°C, 1600°C and 1625°C, respectively. A surprising result was the high temperature (~1600°C) found for MgO-doped Si₃N₄, which was used for comparison.

TABLE 7. CHARACTERISTIC TEMPERATURE FOR THE
ONSET OF DENSIFICATION DURING HOT PRESSING
OF DOPED Si_3N_4

Composition (wt %)	Onset of Densification (°C)	Final Rel. Density (%) (1750°C-55 MPa)
Si_3N_4 (Run 11-13)	>1750	50
$\text{Si}_3\text{N}_4 + 2\% \text{Mg}_3\text{N}_2$	1400	100
$\text{Si}_3\text{N}_4 + 2\% \text{Mg}_2\text{Si}$	1600	99
$\text{Si}_3\text{N}_4 + 1\% \text{Be}_3\text{N}_2$	1625	97.5
$\text{Si}_3\text{N}_4 + 2\% \text{MgO}$	1600	97

finding may suggest that Si_3N_4 powders virtually free of metallic impurities, such as Ca, Al, Fe, etc., require higher hot pressing temperatures to promote densification and consequently, one may expect improved high temperature strength and related properties than observed so far in available forms of hot pressed Si_3N_4 (31).

The mechanism of densification of Si_3N_4 by hot pressing when the nonoxide additives, Be_3N_2 , Mg_2Si and Mg_3N_2 are used has not been investigated. So far, details of the micro-structure, especially the presence of an intergranular phase, have not been resolved. Considerably more information on phase composition during the course of densification must be obtained so that the sequence of events can be described.

SECTION VIII

SINTERING OF Si_3N_4 WITH NON-OXIDE ADDITIONS

A. General

It has been discussed in Sections VI and VII that pure silicon nitride does not respond to either hot-pressing or sintering under conventional conditions.* At 2000°C and above, under 8MPa of N_2 pressure, however, appreciable densification was observed in a limited number of experiments.** Clearly, temperatures above the dissociation temperature at ambient N_2 pressures are necessary to induce sintering. In addition to increased temperature, it is believed that the decreased partial pressure of silicon resulting from increased nitrogen pressure is also essential to bring about densification.

In another series of experiments discussed above, several additions have been identified which induce densification under conventional hot-pressing conditions. The temperatures required to achieve near theoretical densities in amorphous Si_3N_4 with these additions at 55 MPa were about 1750°C . Thus, combining the hyperbaric sintering conditions with the sintering promoting additions, densification was expected at about 200°C above the hot-pressing temperature i.e., somewhere between 1800°C and 2000°C . This has been the case indeed. In addition, many sintering experiments were

* The small shrinkage occasionally observed was attributed to amorphous-crystalline transition in Si_3N_4 .

** Although interference of small amounts of impurities from the furnace could not be excluded.

run at normal pressure of nitrogen. This series of experiments was designed to investigate a broader spectrum of additives than was possible, for scheduling reasons, by hot-pressing. Initial shrinkage in Si_3N_4 with effective sintering promoting additives occurs between 1500°C and 1700°C , i.e., at temperatures not requiring increased nitrogen pressure, and for basic assessment of the effect of an additive such initial shrinkage may be sufficient.

The experiments described above were essentially qualitative in nature and were designed to verify some basic concepts and demonstrate the feasibility of Si_3N_4 sintering. A much broader investigation has to follow before sintering of Si_3N_4 will be available as a process.

B. Experimental

A few gram batches were prepared by mixing In-House Si_3N_4 powders with additives using a mortar and pestle in a nitrogen glove box. Initial dry mixing was followed by homeogenization in a slurry formed by adding a 2% solution of paraffin in benzene. It was believed that the paraffin would help to protect the hygroscopic substances from hydration in air. However, this was not the case, since on exposure to air a pressed pellet containing Mg_3N_2 would fall apart in several hours. Therefore, exposure to air was minimized. The pressing die was loaded in the glove box with dry powder, removed and pressed outside. After ejection the pill was usually immediately repressed isostatically at 200 or 350 MPa and stored in a dessicator above Ca_3N_2 until sintering.

C. Normal Nitrogen Pressure (0.1 MPa) - Results

The various types of chemical additives mixed with fine, amorphous Si_3N_4 powders were (1) nitrides - Be_3N_2 , Mg_3N_2 , AlN , ZrN and Ge_3N_4 , (2) silicides - Mg_2Si , TiSi_2 and B_6Si , (3) elements - B, C, Co and Ni, (4) carbides - ZrC , and (5) combinations of several selected compositions $\text{B}+\text{Be}_3\text{N}_2$, $\text{Be}_3\text{N}_2+\text{Mg}_3\text{N}_2$, $\text{B}+\text{C}$ and $\text{B}+\text{Ni}$. Most compositions contained 1 to 5 wt% additive, separately or in combination.

The powder forming and thermal cycle conditions were similar to those described previously in Section VI-B. Both slow and fast heating rates to firing temperatures between 1750°C and 1800°C were used. Furthermore, a number of experiments were performed by placing the pressed disk of the selected composition into a BN capsule and imbedding the disk completely in Si_3N_4 powder in hope that Si_3N_4 decomposition could be suppressed. In the latter case, the sample was loaded into the BN capsule while in a dry-nitrogen glove box in order to minimize the chance of trapping air, which might possibly interfere with sintering inside the BN capsule.

The major results and conclusions of the investigation of the effect of the above mentioned additives on the sintering behavior of amorphous Si_3N_4 powder in 0.1 MPa (1 atm) of nitrogen pressure can be summarized as follows. Specimens of all compositions underwent high weight losses between 10 and 20% when fired in the open at temperatures between 1750°C and 1800°C. The use of the BN capsule reduced weight losses usually to less than 10%. Hence, the BN capsule partly controlled weight loss due primarily to thermal decomposition. However, the additives had no noticeable effect on the thermal decomposition of Si_3N_4 . Secondly, there was complete absence of shrinkage (hence sintering) for all compositions tried, except for the same three additives, Be_3N_2 , Mg_3N_2 and Mg_2Si , which permitted full densification of Si_3N_4 under hot-pressing conditions. By firing at 1750°C for 15 min in nitrogen, powder compacts of Si_3N_4 (Run 8-10) containing 2% Be_3N_2 , 5% Be_3N_2 , 2% Mg_3N_2 and 3% Mg_2Si gave rise to linear shrinkage values of 3.5%, 4.1%, 3.3% and 4%, respectively. Even under these conditions, the maximum final density of the fired compacts did not exceed 40% of the theoretical value. Apparently, thermal decomposition and the low green density of the compacts inhibit densification, probably due to grain and pore growth. There is little hope that high densities could be obtained at normal nitrogen pressure with the additives investigated, although substantial improvements are anticipated if substantially higher green densities would be used and silicon vapor loss reduced during sintering.

SEM photomicrographs of the microstructures of fired compacts of Si_3N_4 containing 1% B and 3% Mg_2Si are shown in Figures 29(A) and (B) and 30. The boron dopant caused no macroscopic densification, but coarsening of the structure is apparent. Most grains are in the form of equiaxed clusters (Figure 29B) of a variable size range below 1 μ . Individual grains of α - Si_3N_4 , $\sim 0.2 \mu$ in size, appear to exhibit a certain degree of faceting. Thermal grooving between grains is also evident. In Figure 30, the aggregation of grains of Mg_2Si -doped Si_3N_4 into dense clusters is not as apparent. In fact, the individual equiaxed grains of α - Si_3N_4 have better bonding between each other, which is probably the consequence of shrinkage mechanism(s) operating in this case. This explains why fired compacts of Mg_2Si -doped Si_3N_4 were substantially stronger than those of B-doped Si_3N_4 . The microstructures of fired compacts of Be_3N_2 and Mg_3N_2 containing Si_3N_4 were similar to that observed for Mg_2Si -doped Si_3N_4 .

D. Sintering at Hyperbaric Nitrogen Pressure

The sintering was done in a closed-end silicon carbide tube in a furnace described previously by St. Pierre and Curran. For most experiments the pressure of nitrogen was



Figure 29(A). SEM Photo-micrograph of Microstructure of a Compact of SN-402 Si₃N₄ Containing 1 wt% B Fired at 1800°C for 30 Min in N₂ 5500 X

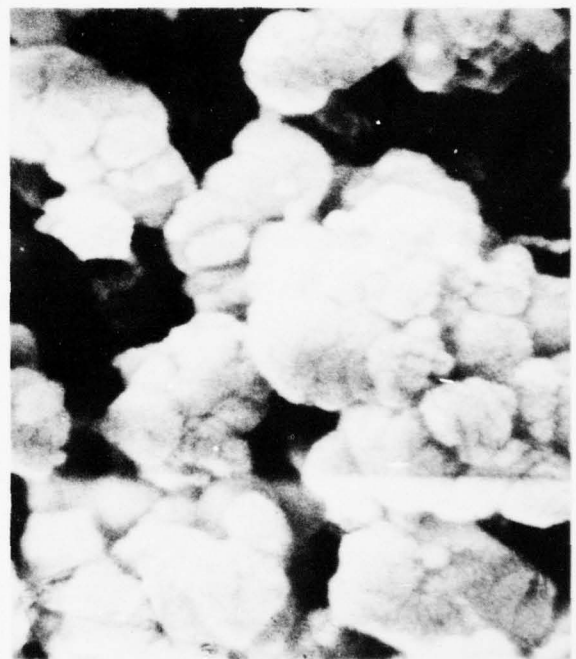


Figure 29(B). SEM Photo-micrograph of Microstructure of a Compact of SN-402 Si₃N₄ Containing 1 wt% B Fired at 1800°C for 30 Min in N₂ 22,000 X



Figure 30. SEM Photomicrograph of Microstructure of a Compact of Run (8-10) Si_3N_4 Containing 3 wt% Mg_2Si Fired at 1750°C - 15 Min - N_2 Mag = 5000 X

selected such that the silicon partial pressure above Si_3N_4 at the sintering temperature, calculated from the free energy of formation, i.e.,

$$P_{\text{Si}} = \left(\frac{e^{-\Delta G_f}}{\frac{kT}{2} P_{\text{N}_2}} \right)^{1/3}$$

would be equal to or less than the silicon vapor pressure above SiC . It was hoped that in this way the silicon loss from the sintering specimens would be sufficiently suppressed. Although this was effective it was not sufficient enough, and in later experiments the pill in the muffle was loosely packed in Si_3N_4 powder* which brought about additional improvements in sintering.

Temperature was measured by an L&N optical pyrometer at the closed end of the tube, corrected for furnace window absorption and a mirror. Readings were believed accurate within $\pm 25^\circ\text{C}$, with positive deviations more likely due to occasional light fogging of the furnace window. "High Purity Dry Nitrogen" from Union Carbide Company was used as the furnace atmosphere. No analysis of the gas was available. The system was kept under vacuum while the temperature was brought up to 800°C , and was pressurized at that point.

*Silicon Nitride Electronic Grade Apache Chemicals Inc.

1. Results

The specimens were evaluated primarily in terms of shrinkage and density obtained by water displacement. The initial specimens were nonuniformly sintered (tapered), either due to temperature gradients or perhaps silicon vapor pressure gradients; for such specimens the longitudinal shrinkage is given. Most of the specimens were sectioned and polished for metallography. However, etching to reveal grain morphology turned out to be a difficult task, and there was not enough time during this program to work out the proper technique. Thermal etchings were unsuccessful. Some results were obtained by etching (1) in molten NaOH at about 250°C for 3 to 5 min, and (2) in hot NH₄F + HNO₃ for 10 to 15 min. However, the specimens overetch easily because of the very fine grain size. Therefore, only few examples of grain structure are given below.

The results of the most important experiments are collected in Table 8. Observation of the data suggests several trends in the behavior of Si₃N₄ under hyperbaric sintering conditions. Primarily all the additions which brought about densification on hot-pressing also promoted sintering. The combined Be₃N₂-Mg₃N₂ additions seemed to be more effective than any other addition tested and the majority of experiments were done, therefore, with a 1:2 ratio of this combination. No other ratio or concentration has been investigated. It is likely that smaller additions would also be effective.

In experiments 1-5 (Table 8) nonuniform shrinkage was observed, the specimens were tapered and the opposite faces showed different degrees of densification. This could be almost eliminated by packing the specimens in loose Si₃N₄ powder during firing in experiments 6-15.*

Experiments 3-7 indicate that increased temperature and green density increase the degree of densification, a quite predictable result, and also that increased nitrogen pressure increased density (Exp. 4-5).

The green densities of the compacts were low, even after compaction at 350 MPa as a result of the low specific weights of the amorphous powders. Calcination of the powders to 1150° and 1480° brought substantial improvements, both in green and fired densities.

* Whether the merit of the powder used for covering of the pill during sintering was to remove temperature gradients or retard evaporation has not been positively determined.

TABLE 8. RESULTS OF HYPERBARIC SINTERING EXPERIMENTS

Exp. No.	Si ₃ N ₄ Powder* Code	Addition Wt. %	Approx. Green Density %	Sintering Conditions			Shrink. %	Weight Loss %	Density g/cc	Comment
				T°C	t min	PN ₂ (MPa)				
1	8-10	Mg ₃ N ₂ 5	33	1680	10	5.5	~8	n.d.	n.d.	non uniform shrinkage
2	"	"	33	1750	11	5.5	~11	n.d.	n.d.	"
3	11-13	Be ₃ N ₂ 1 Mg ₃ N ₂ 2	35	1700	10	5.5	~15	n.d.	n.d.	"
4	"	"	37	1750	15	2.85	15	n.d.	1.95	62
5	"	"	37	1750	15	7.2	21	n.d.	2.4	75
6	"	"	37	1750	15	7.5	22	n.d.	2.6	82
7	"	"	45	1800	10	8.5	21	2	2.99	94
8	16-15	"	45	1850	15	7.5	25	12	2.95	93+
9	"	"	44	1880	30	7.8	26	11	3.11	98
10	17	"	46	1850	20	8.5	19.5	6	n.d.	Fig. 33
11	"	"	46	1950	20	8.5	19.5	6	n.d.	strong disruption see text and Fig. 31
12	"	"	51	1880	20	8.5	19.5	6	2.93	93
13	"	"	51	2000	20	8.5	21.0	6	3.12	98
14	"	Mg ₃ N ₂ 2	47	1950	20	8.5	18	7	2.56	Figs. 34-36
15	8-10	Mg ₂ Si ₃	n.d.	1750	95	8.5	12	1	1.8	"
										"

*Table

**Specimen covered by Si₃N₄ powder during sintering in Exp. 6-15.

The results further indicate that the weight loss is about constant for a given batch of powder and therefore it relates, more likely, to the chemistry of the powder than to the sintering conditions. In fact it reflects the sum of three or four components; evaporation of paraffin used as the binder (about 3%), loss of weight due to release of ammonia from the amorphous Si_3N_4 (see above), weight loss due to thermal decomposition of Si_3N_4 during sintering, and weight gain due to nitridation of hyperstoichiometric silicon.

In several experiments it was observed that the sintered specimen was densified but disrupted by a network of cracks, as shown in Figure 31. This effect was particularly strong with powder No. 17 (experiments 10, 11). It was suspected that this cracking occurred during the exothermic crystallization of the amorphous Si_3N_4 at 1480°C . Therefore, the prepared powder with the additives was calcined to 1480° in experiments 12 and 13. At this calcination temperature, crystallization was barely detectable by X-rays i.e., the crystallite size was very small. Compacts sintered using the calcined powders did not crack. However, the temperature to obtain the same final density as with a noncrystalline powder was somewhat greater, by about 100°C (compare experiments 9, 12 and 13).

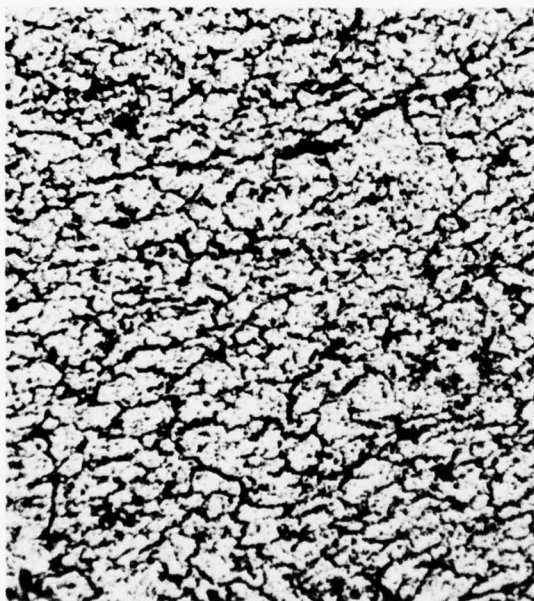


Figure 31. Sintered Si_3N_4 Disruption of Specimen Due to Amorphous-Crystalline Transition 55 X

2. Microstructures

Figures 32(A), (B) show photomicrographs of specimen 6, the first specimen which was successfully sintered to an appreciable density, 82%. The optical micrograph was taken near the periphery of the section where the density was higher than average. The relatively large pores are due, in part, to the insufficient processing and the low green densities. Nevertheless, one observes in the section sizable areas of very high density, a quite encouraging feature in the quest for a new sintering process. The scanning electron micrograph in Figure 32(B) shows the fracture surface of the same specimen. The structure is composed of essentially equiaxed grains around one micron in size with the largest grains about 2 microns. One observes faceting and grain boundary grooving in the pores.

Comparing the grain size of this specimen with that estimated for Si_3N_4 consolidated at 1550°C under diamond forming conditions (Figure 12), one concludes that substantial grain growth occurred during sintering at 1750° with additives. This observation, along with the absence of grain growth on annealing of the undoped high pressure hot-pressed Si_3N_4 at 1750°C (Figure 13), suggests that the sintering additives may have increased the mass transport rate(s) (volume or grain boundary diffusivity).

Figure 33, an optical micrograph of a polished section of specimen number 9 sintered at 1980°C , demonstrates the very low porosity achievable in Si_3N_4 on hyperbaric sintering. The scanning electron micrograph in Figure 34 shows the surface of a polished (and etched) section of specimen No. 13 (Table 8). The photographed area is essentially pore free, however, the specimen did contain some pores and imperfections due to processing. Nevertheless, this result proves that Si_3N_4 with additives can be sintered close to theoretical density. The etchant was a mixture of HF, HNO_3 and H_2O_2 , and obviously, did not attack the surface. Molten NaOH at about 250°C did etch the surface, however, little could be resolved unless the specimen was severely overetched. This was due to poor contrast resulting from the light tan color of the specimen and the very fine grain size. In the NaOH etched surface, optical microscopy resolved elongated grains, some up to about 30 microns long with an aspect ratio of about 5 to 8, embedded in a finer matrix which could not be resolved (Figure 35). Figure 36 shows an SEM micrograph of the elongated, prismatic grain morphology taken from the same overetched surface. The grains here are typically 1-2 microns thick and 3 to 10 microns long. It is probable that still finer grains were etched away. At a

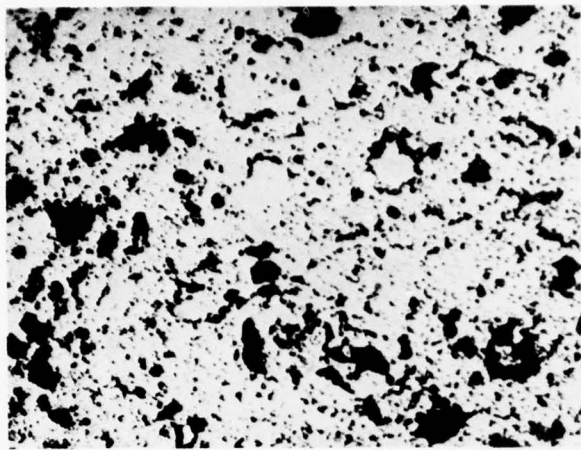


Figure 32(A). First
 Si_3N_4
Speci-
men
Sin-
tered
to Ap-
pre-
ciable
Density
(Exp.
No. 6
Table
8) Opti-
cal
Micro-
graph
of Sec-
tion
580 X

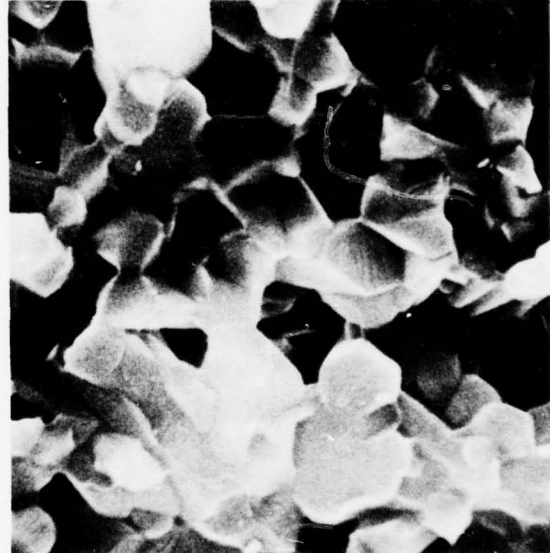


Figure 32(B). First Si_3N_4
Specimen Sin-
tered to Ap-
preciable
Density (Exp.
No. 6, Table 8)
SEM of Fracture
Surface 10,000 X



Figure 33. Si_3N_4
Sintered
at 1880°C
and 8 MPa
 N_2 to 98%
Density
500 X



Figure 34. SEM of Polished
Section of Specimen
No. 13 2200 X

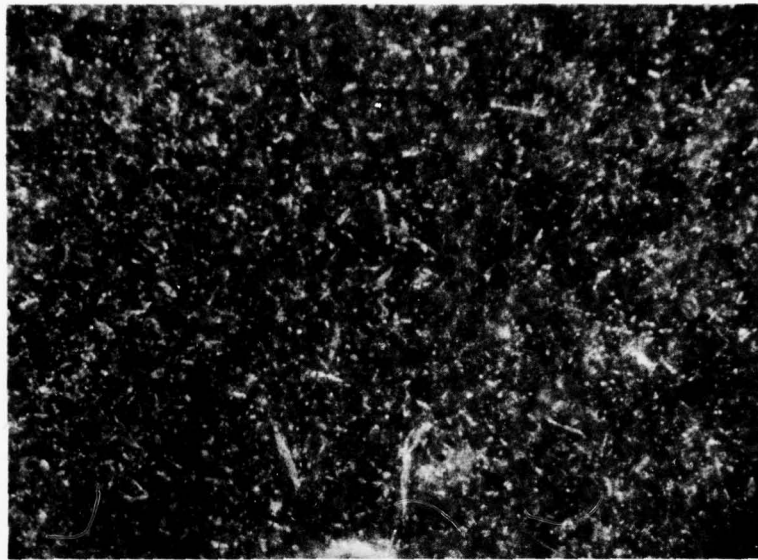


Figure 35. Section of Specimen 13 Etched with NaOH Incident Light, 580 X

higher magnification (Figure 37), one can see that some of the prismatic grains are faceted and have hexagonal cross sections.* The grain morphologies of specimens 9 and 13 reveal that increasing the sintering temperature to 2000°C brought about strong anisotropic grain growth in this composition. Similar grain shape has been observed before in Si_3N_4 hot-pressed with MgO additions at temperatures near 1800°C³²) and also in pure Si_3N_4 exposed to 1820°C. The sintering behavior of silicon nitride under hyperbaric nitrogen conditions, as observed in the above experiments, may be summarized as follows:

- (1) The degree of densification increases with temperature, nitrogen pressure and green density.
- (2) 98% of theoretical density was obtained with $\text{Be}_3\text{N}_2 + \text{Mg}_3\text{N}_2$ additives (1+2%) in small specimens at 1880°C and above and 8 MPa of nitrogen.
- (3) Amorphous Si_3N_4 powders yield low green densities and tend to introduce severe cracking due to the exothermic amorphous-crystalline transition.

* It has been determined with another specimen by electron diffraction that the grains are elongated in the c-direction.



Figure 36. Surface of Overetched Specimen 13 SEM, 2200 X



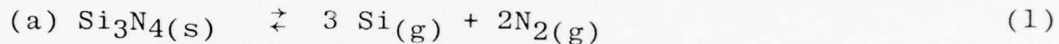
Figure 37. Morphology of Grains in Si_3N_4 Sintered at 2000°C SEM, 10,000 X

(4) Si_3N_4 sintered at or above about 1900° exhibits anisotropic grain growth. $\beta\text{-Si}_3\text{N}_4$ grows in the c-direction and forms prismatic grains with an aspect ratio up to 8.

E. Discussion

The peculiarities of the sintering of Si_3N_4 , such as lack of bonding and densification, cessation of shrinkage, sensitivity to the heating rate⁽¹⁰⁾ etc., are related to its thermal decomposition, a phenomenon absent during sintering of many other typical ceramics. In order to understand its effect, one has to consider the interference of the thermal decomposition with the internal transport mechanisms responsible for sintering. The following will give a qualitative picture of this interaction as we presently understand it.

Thermal decomposition of Si_3N_4 is described by the reaction;



$$(b) P_{\text{Si}} = \left(e^{\frac{-\Delta G_f}{kT}} \right)^{1/3} P_{\text{N}_2} \quad (2)$$

where ΔG_f is the sum of the free energy of formation at T and the latent heat of the $3\text{Si}(\text{l}) \rightarrow 3\text{Si}(\text{g})$ transition. Thus P_{Si} , the silicon vapor pressure above a silicon nitride surface, is fixed by the ambient nitrogen pressure. As long as P_{Si} is less than the saturated vapor pressure above silicon at T, which is true for all practical situations, there is no condensed silicon present and whether or not reaction (1) proceeds depends on the removal of silicon vapor from the system. Because there is no practical means to prevent the escape of silicon vapor, thermal decomposition will always occur. It is the consequence of thermal gradients in a furnace which necessarily impose silicon vapor pressure gradients and bring about transport of silicon away from a specimen positioned in the hot zone.

The rate of thermal decomposition in a powder compact may be controlled by one of three steps:

- (1) rate of reaction,
- (2) transport of the gaseous species through pores, or
- (3) transport of Si vapor away from the outer surface of the specimen.

Experimental evidence obtained in this work indicates that step one has been rate controlling, at least in some experiments. It follows from the relationship between specific surface area and weight loss observed during heat treatment of powder compacts in various atmospheres. If step two were controlling evaporation, the weight loss would be proportional to the porosity i.e., slightly increasing as porosity goes up due to evaporation. This has not been observed. The same argument excludes step three as rate controlling in our experiments. In addition, if the migration through the pores controlled the rate, the outer geometrical surface would evaporate faster and a dimensional change would be expected. This has not been the case.

The thermal decomposition is, however, a reversible process, and recombination of $Si_{(v)}$ and N_2 into Si_3N_4 will occur within the pores of the powder compact as a result of local variations of P_{Si} . This silicon pressure, as expressed in equation (2), is that over a flat surface. It is affected by surface curvature K , such that P_{Si}^1 above a curved surface is:

$$P_{Si}^1 = P_{Si} e^{\frac{K\gamma\Omega}{kT}}$$

where γ is surface energy and Ω molar volume. P_{Si}^1 varies with K , the local curvature in the pores, and consequently, there is internal material transport due to thermal decomposition and recombination, proceeding from loci of positive curvature to loci of negative curvature. The terms "positive" and "negative" here are relative, i.e., with respect to the mean average curvature \bar{K} of the internal surface S , where \bar{K} is

$$\bar{K} = \frac{1}{S} \iint K \Delta S$$

In a very simplified way, one can look at this process as matter transport from large pores into small pores. Thus, large pores grow and smaller ones are filled in, resulting in the formation of a structure composed of large polycrystalline domains separated by large pores, as described by Greskovich and Rosolowski(33), the dense domains being interconnected by relatively narrow bridges.*

When now, in the case of Si_3N_4 , material loss from the system is superimposed on the process of coarsening, the narrow bridges connecting the solid domains tend to evaporate preferentially, as they have the highest positive curvature, and the system undergoes disconnection into separate poly-

* This process, designated as coarsening, is manifested by a decrease in specific surface area.

crystalline particles. This is manifested by the familiar loss of coherence and strength in Si_3N_4 compacts exposed to high temperatures at normal nitrogen pressure.

What happens when the temperature is increased such that additional transport mechanisms (volume and grain boundary diffusion, liquid phase assisted material transport) start to operate depends on:

- (1) the degree of disconnection which the system previously suffered and;
- (2) the ratio of the rate of matter transport due to thermal decomposition-recombination to that due to volume, grain boundary and liquid transport (transport mechanisms leading to densification). If the system was severely disconnected by the time it reached the sintering temperature, no densification can occur, because whatever changes go on proceed within the separated parts of the system. The lack of connectivity excludes coordinated movement of the parts, and shrinkage is not observed.

If the system was not seriously affected by disconnection and coarsening when densification started to operate, then shrinkage proceeds. The final outcome in this latter case depends on the competition of the two kinds of atomic transport mechanisms, those which do and those which do not densify the system. These, in turn, are primarily dominated by their activation energies.

From the above analysis it seems that there are three ways to affect sintering of silicon nitride:

- (1) Enhance volume, grain boundary or liquid assisted mass transport.
- (2) Suppress thermal decomposition.
- (3) Suppress coarsening of the system.

The first is accomplished by using very fine particles and by chemical activation through additives. Also, high green densities may be expressed in these terms; increased compaction decreases diffusion distances and increases initial curvature gradients.

The second approach, at least in principle, can be achieved by preventing silicon loss during sintering.

Both 2 and 3 may be achieved by decreasing the equilibrium Si pressure above the Si_3N_4 surface by raising the nitrogen pressure in the sintering atmosphere.

REFERENCES

1. B.D. Powell and P. Drew, "The Identification of a Grain-Boundary Phase in Hot-Pressed Silicon Nitride," *J. Mat. Sci.*, 9 1867 (1976).
2. S.U. Din and P.S. Nicholson, "Creep Deformation of Reaction-Sintered Silicon Nitrides," *J. Amer. Ceram. Soc.*, 58 (11-12) 500 (1975).
3. G. Gazza, "Hot Pressed Si_3N_4 ," *J. Amer. Ceram. Soc.*, 56 (2) 662 (1973).
4. K.S. Mazdynasni and C.M. Cooke, "Consolidation, Microstructure and Mechanical Properties of Si_3N_4 Doped with Rare-Earth Oxides," *J. Amer. Ceram. Soc.*, 57 (12) 536 (1974).
5. R.W. Rice and W.J. McDonald, "Hot-Pressed Si_3N_4 with Zr-Based Additions," *J. Amer. Ceram. Soc.*, 58 (5-6) 264.
6. A. Tsuge, K. Nishida and M. Komatsu, "Effect of Crystallizing the Grain-Boundary Glass Phase on the High Temperature Strength of Hot-Pressed Si_3N_4 Containing Y_2O_3 ," *J. Amer. Ceram. Soc.*, 58 (7-8) 323 (1975).
7. R. Rice, personal communication, 1976.
8. S.C. Singhal, "Thermodynamics and Kinetics of Oxidation of Hot-Pressed Silicon Nitride," *J. Mat. Sci.*, 11 500 (1976).
9. F.F. Lange, S.C. Singhal and R.C. Kusuicki, "Phase Relations and Stability Studies in the Si_3N_4 - SiO_2 - Y_2O_3 System," Tech. Report Contract No. N00014-74-C-0284, Westinghouse Electric Corp., (1976).
10. G.R. Terwilliger and F.F. Lange, "Pressureless Sintering of Si_3N_4 ," *J. Mat. Sci.*, 10 1169 (1975).
11. M. Mitomo, "Pressure Sintering of Si_3N_4 ," *J. Mat. Sci.*, 11 1103 (1976).
12. G.R. Terwilliger, "Properties of Sintered Si_3N_4 ," *J. Amer. Ceram. Soc.*, 57 48 (1974).
13. T. Buljan, presentation at the 1976 Americal Ceramic Society Convention.
14. Isao Oda, private communication, 1976.
15. B.F. Jones and M.W. Lindley, "Additional Observations on the Strength/Nitrided Density Relationship for a Reaction Sintered Silicon Nitride," *J. Mat. Sci.*, 11 191 (1976).

16. C. Greskovich, J.H. Rosolowski and S. Prochazka, "Ceramic Sintering," ARPA Final Technical Report, General Electric Report No. SRD-75-084, 1975.
17. T.R. Wright and D.E. Niesz, "Improved Toughness of Refractory Compounds," NASA Report No. CR-134690, (1974).
18. D.R. Stull and H. Prophet, JANAF Thermochemical Tables, second edition, NSRDS-NBS 37, June 1971.
19. K.S. Mazdiyasni and C.M. Cooke, "Synthesis, Characterization and Consolidation of Si_3N_4 Obtained from Ammonolysis of $SiCl_4$," J. Amer. Ceram. Soc., 56 628 (1973).
20. G.G. Deeley, "Bonding Si_3N_4 to Strong Dense Ceramics," Brit. Patent 970639, 1964.
21. P.E.D. Morgan, "Production and Formation of Si_3N_4 from Precursor Materials," Final Report (ARPA) A-C3316, Dec. 1976.
22. V.Y. Doo, D.R. Kerr and D.R. Nichols, "Property Changes in Pyrolytic Si_3N_4 with Reactant Composition Changes," J. Electrochem. Soc., 115 61 (1968).
23. E.A. Taft, "Characterization of Silicon Nitride Films," J. Electrochem. Soc., 118 1342 (1971).
24. Y. Watanabe, "Molecular Structure and Cracks of Films Formed from SiH_4 and NH_3 ," Japan J. Appl. Phys., 7 960 (1968).
25. K. Niihara and T. Hirai, "Chemical Vapor Deposition of Si_3N_4 ," J. Mat. Sci., 11 592 (1976).
26. Handbook of Chemistry and Physics, 53rd edition, Edit. by Robert C. Weast, pub. by The Chemical Rubber Co., Cleveland, Ohio (1972-73).
27. B.J. Wuensch and T. Vasilos, "Self Diffusion in Silicon Nitride," Final Report (ARPA), Contract No. N00014-73-C-0212, March 1975.
28. J. Nadeau, "Very High Pressure Hot Pressing of SiC ," Bull. Am. Ceram. Soc., 52 170 (1973).
29. H.T. Hall, "Ultra High Pressure, High Temperature Apparatus - The Belt," Rev. Sci. Inst., 31 125 (1960).
30. R.J. Lumby and R.F. Coe, "The Influence of Some Process Variables on the Mechanical Properties of Hot-Pressed Silicon Nitride," Proc. Brit. Ceram. Soc., 15 91-101 (1970).

31. D.W. Richerson, "Effect of Impurities on the High Temperature Properties of Hot-Pressed Silicon Nitride," Bull. Am. Ceram. Soc., 52(7) 560-62 (1973).
32. G.R. Terwilliger and F.F. Lange, "Hot Pressing Behavior of Si_3N_4 ," J. Mat. Sci., 57 25 (1976).
33. C. Greskovich and J.H. Rosolowski, "Sintering of Covalent Solids," J. Amer. Ceram. Soc., 59 336 (1976)